Forside

Eksamensinformation
NPLK16801E - Environmental Science Thesis 45 ECTS, Department of Plant and Environmental Sciences - Kontrakt:142587 (rxc482)

Besvarelsen afleveres af
rxc482 rxc482
rxc482@alumni.ku.dk

Eksamensadministratorer
Eksamensteam, tel 35 33 64 57
eksamen@science.ku.dk

Bedømmere
Tue Kjærgaard Nielsen
Eksaminator
tkn@plen.ku.dk
+4535324188

Jens Aamand
Censor
jeaa@geus.dk

Besvarelsesinformationer

Titel: Investigating Potential PFAS Degradation by Environmental Microorganisms via Colorimetric Screening Assay
Titel, engelsk: Investigating Potential PFAS Degradation by Environmental Microorganisms via Colorimetric Screening Assay
Tro og love-erklæring: Ja
Indeholder besvarelsen fortroligt materiale: Nej
Må besvarelsen gøres til genstand for udlån: Ja

UNIVERSITY OF COPENHAGEN
FACULTY OR DEPARTMENT

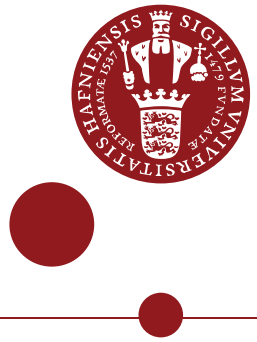

A thesis submitted to the Department of Plant and Environmental Sciences at the University of Copenhagen

Master of Environmental Science

Investigating Potential PFAS Degradation by Environmental Microorganisms via Colorimetric Screening Assay

Annaliese Nan Vernon

rxc482@alumni.ku.dk

Supervisors: Tue Kjærgaard Nielsen and Asal Forouzandeh

Submitted on 31 May, 2024

Table of Contents

Acknowledgments

Thank you to Tue K. Nielsen for the opportunity to work on this exciting project. I enjoyed this chance to try something new under your guidance. Many thanks to Asal Forouzandeh for working with me nearly every step of the way, it was great being in the lab and doing the sampling portion of this project with you. I am very grateful to Ulla Rasmussen and Dorthe T. Ganzhorn for their help in the lab. A big thanks to Lars H. Hansen and all the kind people of the Environmental Microbial Genomics group for being so welcoming. I learned so much from all of you. Lastly, this thesis wouldn't have been possible without the support of my amazing friends and family, both in Copenhagen and at home. Thank you all for listening to me talk about this thesis for the last months and for the many words of encouragement you provided along the way.

Declaration

Much of the work for this thesis was done in close collaboration with Asal Forouzandeh. This includes the sampling, the positive control defluorination experiment, and the colorimetric assay. The nanopore sequencing was completed with assistance from Tue K. Nielsen. Initial data processing for the gene sequences was completed by Tue K. Nielsen. The chemical analysis work and initial data treatment were performed by Martin Hansen. All other aspects of the work for this thesis were completed by the undersigned.

Abstract

Public concern over the pervasive distribution and associated risks of ‘forever chemicals’ to human and environmental health has been growing. A sustainable and effective degradation mechanism for such perfluoroalkyl and polyfluoroalkyl substances (PFAS) is relevant to managing these recalcitrant pollutants found in diverse environments across the globe. Bioremediation of PFAS is an option worth exploring. Microorganisms isolated from contaminated sites could be a source of the biological machinery and associated genetics to confront such a task. This thesis investigates the capacity of bacteria from PFAS-contaminated environments in Denmark to break down perfluorooctanoic acid (PFOA) using a colorimetric screening assay that changes color upon contact with free fluoride. Genetic sequencing of the samples showed several bacteria that had previously been noted for their biodegradation abilities, including *Pseudomonas fluorescens*, *Delftia acidovorans*, *Paraburkholderia fungorum*, and *Stenotrophomonas maltophilia*. Chemical analysis of the samples with environmental bacteria showed significant PFOA reduction compared to the non-bacteria control. However, the fate of the PFOA in this project remains unconfirmed. This research shows promising potential for the screening method. Future studies are needed to further understand PFAS biodegradation potential.

1. Introduction

1.1 Defining Perfluoroalkyl and Polyfluoroalkyl Substances (PFAS)

Perfluoroalkyl and polyfluoroalkyl substances, also known as PFAS, are a subset of anthropogenic fluorinated compounds consisting of an aliphatic carbon chain where some or all the hydrogen substituents have been replaced with fluorine, typically with the chemical structure C_nF_{2n+1}−R (Buck et al., 2011; Wang et al., 2017). As initially defined by Buck et al. in 2011, **perfluoroalkyl** compounds have all the positions occupied by hydrogen atoms on the hydrocarbon equivalent filled instead with fluorine atoms, except those associated with functional groups (Buck et al., 2011). In **polyfluoroalkyl** substances, fluorine has replaced hydrogen on at least one, but not necessarily all, of the carbons in the alkyl chain, resulting in a partially fluorinated compound that may still have some hydrogens attached. In 2021, the PFAS definition was expanded by the Organization for Economic Cooperation and Development (OECD), which defined PFAS as "fluorinated substances that contain at least one fully fluorinated methyl or methylene carbon atom (without any H/Cl/Br/I atom attached to it), with noted exceptions for any chemical with at least a perfluorinated methyl group ($–CF_3$) or a perfluorinated methylene group ($–CF_2–$), is a PFAS" (OECD, 2021).

Key subcategories of PFAS include perfluoroalkyl sulfonic acids (PFSAs) and perfluoroalkyl carboxylic acids (PFCAs), which are distinguished by their functional groups. PFSAs have a sulfonic acid group ($C_nF_{2n+1}SO_3H$) [e.g., perfluorooctane sulfonic acid (PFOS)], and PFCAs have a carboxylic acid group ($C_nF_{2n+1}COOH$) [e.g., perfluorooctanoic acid (PFOA)] (Buck et al., 2011). Both PFSAs and PFCAs fall into the category perfluoroalkyl acid (PFAA), which, along with PFAA precursors, polyfluoroalkyl acids, and "other PFAS," are the primary PFAS families (OECD, 2021).

PFAS are further distinguished by the length of their carbon chain due to the varying toxicity and bioaccumulation potential between long-chain and short-chain PFAS. PFCAs with carbon chain lengths of eight and greater and PFSAs with carbon chain lengths of six and greater qualify as long-chain PFAS (Buck et al., 2011).

PFAS is a broad class of chemicals encompassing a diverse range of molecular structures with varying physical, chemical, and biological properties. The reactivity, solubility, molecular weight, and bond strength of PFAS vary considerably (Evich et al., 2022). This thesis focuses on PFAS and other fluorinated compounds that may not meet the direct definition of PFAS but contain the relevant C-F bond, therefore falling into the category of perfluorinated chemicals (PFCs). The electronegativity of fluorine and its small size make the carbon-fluorine bond exceptionally strong, with a bond strength of 450kJ/mol (Krafft & Riess, 2015). This characteristic leads fluorinated compounds to exhibit low reactivity, making them desirable for manufacturing due to their durability. However, this attribute also poses a challenge in the degradation process, as evidenced by the colloquial term for PFAS, “forever chemicals.”

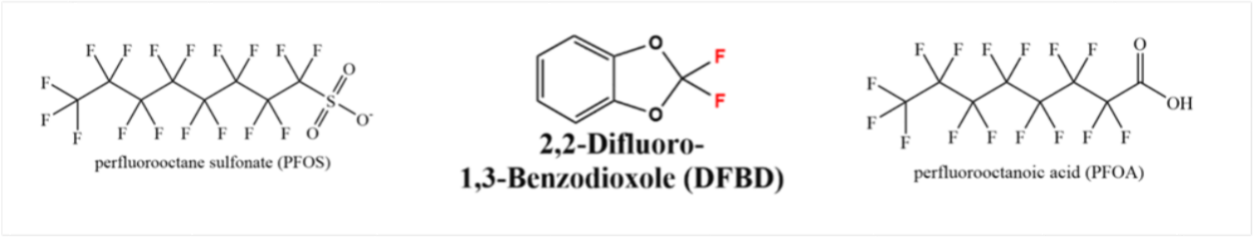

Figure 1: Relevant fluorinated compounds. PFOS (CAS #1763-23- 1) and PFOA (CAS #335-67-1) are the classic long-chain PFAS. DFBD is not a PFAS but is relevant to this study.

1.2 History of PFAS

PFAS were first synthesized in the late 1930s, and their development continued into the 1940s, consisting of two main processes: electrochemical fluorination (ECF) and fluorotelemorization (ITRC, n.d.). By the 1950s, manufacturing and commercial production of various PFAS started to escalate. PFAS tend to be excellent surfactants and simultaneously hydrophobic and oleophobic (ITRC, n.d.). Additionally, they are chemically and thermically stable, making them long-lasting and unlikely to break down, even under stressful conditions and over long timescales (ITRC, n.d.).These properties brought PFAS into an array of industries, including aviation, construction, electronics, firefighting, and various medical applications (ITRC, n.d.). Additionally, PFAS are, and have been, used in various consumer products such as food packaging, non-stick cookware, furniture, carpets, waterproof clothing, and outdoor equipment (ITRC, n.d.; Lindstrom et al., 2011). Over 8,000 unique chemical structures of PFAS are used in over 200 applications (Evich et al., 2022).

In the decades between the 1970s and 1990s, several studies identified PFOA, among other fluorinated chemicals, in human blood samples (Lindstrom et al., 2011). Between 2000 and 2002, the US Environmental Protection Agency (EPA) worked with the major chemical manufacturer, 3M, to discontinue production of many long-chain PFAS compounds (Lindstrom et al., 2011). PFAS were further restricted in the United States through the 2006 PFOA Stewardship Program which further reduced production of long-chain PFCAs and related precursors (ITRC, n.d.). In the European Union, PFOS and its derivatives were restricted by Regulation (EC) No 850/2004 to comply with provisions in the Stockholm Convention on Persistent Organic Pollutants (Lassen et al., 2013). However, as of 2018, the OECD/UNEP Global PFC Group still found over 4,730 PFAS with registered CAS numbers (OECD, 2021). Furthermore, a 2020 technical report by the Clean Energy Manufacturing Analysis Center found that over a megaton of PFAS is produced per year on a global scale (Booten et al., 2014).

Recent efforts have focused on finding alternatives to many of the longer-chain PFAS that were restricted during the 2000s and have documented toxicity. However, these alternatives are often just shorter-chain PFAS (Evich et al., 2022). While shorter-chain PFAS tend to get eliminated from living organisms faster, there is still evidence for toxicological concern (Mahoney et al., 2022). Such shorter-chain PFAS have also been shown to accumulate in plants, which could cause an increase in human dietary exposure (EEA, 2019). Overall, PFAS remain a concern for both citizens and governments due to their persistence in the environment, their global

prevalence, and their toxicological implications. In January of 2023, Denmark, in collaboration with Germany, the Netherlands, Sweden, and Norway, submitted a proposal to restrict the manufacturing, sale, and use of PFAS in the EU under the REACH (Registration, Evaluation, Authorization and Restriction of Chemical Substances) (ECHA, 2023).

1.3 Toxicology of PFAS

The widespread use of PFAS and their inherent properties leading to degradation resistance has dual implications for their persistence both in the environment and the human body, where their long biological half-life leads to bioaccumulation and risk of toxicological effects. PFAS have been found in the blood of nearly all populations tested in developed countries, with one study conducted between 1999 and 2008 finding PFOS, PFOA, PFNA, and PFHxS in more than 95% of serum samples taken from participants representing the general US population over 12 years of age (Kato et al., 2011).

Epidemiological studies have shown associations between various PFAS and toxicological endpoints, such as lower immune function, thyroid, kidney, and liver diseases, lipid and insulin dysregulation, altered reproductive/developmental outcomes, and even certain cancers (Fenton et al., 2021). Elevated PFAS levels in blood correlate with reduced measurements of biomarkers indicative of healthy immune response (Fenton et al., 2021). A related association has been shown between high PFAS concentrations in serum and reduced vaccine efficacy, as well as higher rates of thyroid disease, which is a condition connected to autoimmune response (Fenton et al., 2021). PFAS are also associated with adverse reproductive consequences, including reduced sperm motility and concentration in men and increased fecundity (time until pregnancy) in women (Fenton et al., 2021). Additionally, PFAS have been shown to cross the placenta and enter breast milk (Starling et al., 2020). One epidemiological study with schoolchildren from the Odense Child Cohort in Denmark conducted between 2010 and 2020 found an association between higher concentrations of certain PFAS in maternal blood and lower Full Scale Intelligence Quotient (FSIQ) scores from their children at age 7 (Beck et al., 2023).

Animal studies using rats and mice have shown related effects, such as increased liver weight, disturbed thyroid hormone levels, disturbed lipid metabolism, impaired mammary gland development in mice, and tumor induction in rodents (Schrenk et al., 2020). The characterization of risk from PFAS is likely to differ based on exposure levels, sex, and stage of life during

exposure. Both epidemiological and animal studies raise concerns over PFAS as they have been found to have endocrine-disrupting, immunotoxin, neurotoxic, and carcinogenic effects (Boyd et al., 2022; Fenton et al., 2021). Additionally, in 2019, the European Food Safety Authority (EFSA) identified the "mixture effect" as a critical toxicological consideration, meaning the combined impact of PFAS compounds could be heightened compared to their toxicity alone due to their shared toxicokinetic properties and long half-lives (Schrenk et al., 2020).

The classic PFAS that have been manufactured for a longer amount of time, known as "legacy compounds" (e.g., PFCAs and PFSAs), have been evaluated for toxicology and found to be harmful. However, toxicology studies have lagged behind the development of newer PFAS compounds, many of which remain poorly characterized and have impacts on health that are not fully understood, especially when considering the mixture effect (Evich et al., 2022; Wang et al., 2017).

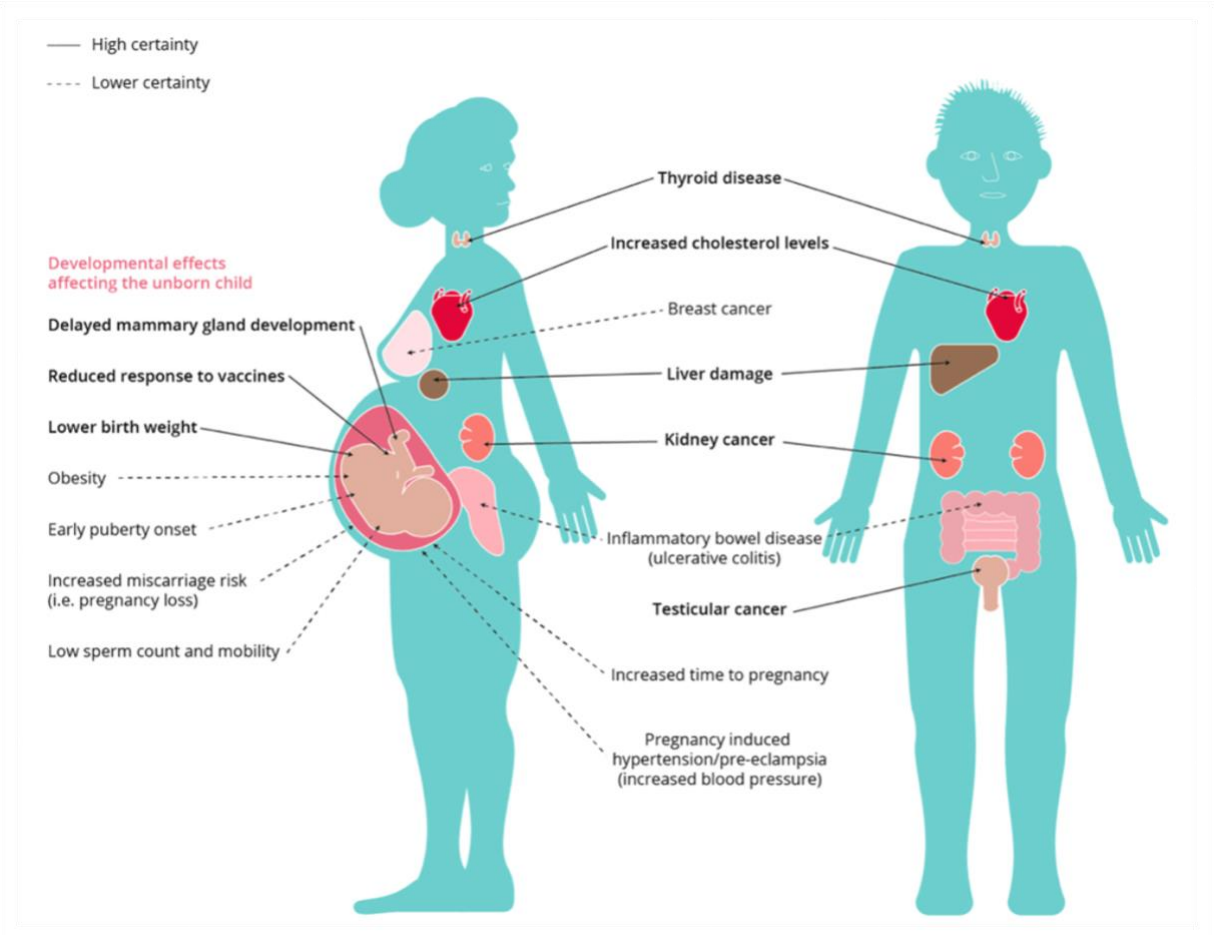

Figure 2: Toxicological Endpoints of PFAS Exposure. As published by the European Environment Agency (EEA, 2019).

1.4 Environmental Prevalence of PFAS

PFAS pollution is relevant beyond the human body and human society, as this class of chemicals has been detected in a diverse array of environmental samples collected across the globe. PFAS distribution is often described as ubiquitous. PFAS and their degradation products have been found in a wide range of biota, including fish, birds, dolphins, pandas, and polar bears (Rekik et al., 2024; Vendl et al., 2024). PFAS tend to follow biomagnification processes and are often found in higher quantities at higher trophic levels (Evich et al., 2022). These substances have also been documented in diverse ecosystems ranging from urban water runoff to remote lands, such as the Arctic (Garnett et al., 2021) (Larsen & Giovalle, 2015). The physical-chemical properties of specific PFAS compounds, as well as how they were released, affect the fate of the chemicals. Longer-chain PFAS and those with sulfonate groups, rather than carboxylate groups, tend to sorb more readily to soils (Shahsavari et al., 2021). Direct release of PFSAs and PFCAs into aquatic ecosystems results in their widespread distribution, whereas volatile precursors like fluorotelomer alcohols (FTOHS) or the shorter-chain new-generation PFAS can be transported via atmospheric systems (Evich et al., 2022; Mahoney et al., 2022; Routti et al., 2017).

The actual pollution load of PFAS is likely underestimated due to the lack of standards to detect PFAAs using targeted analysis methods (Liu & Mejia Avendaño, 2013). Many PFAS precursors are released, transported, and eventually transformed by processes like hydrolysis, oxidation, reduction, decarboxylation, and hydroxylation in the environment, ultimately yielding stable PFAS (Evich et al., 2022). This phenomenon explains why PFOA and PFOS are often detected at higher levels in wastewater effluent than influent, as the PFAS precursors frequently go undetected until their transformation (Liu & Mejia Avendaño, 2013). The majority of PFAS compounds ever produced fall into the category of PFAS precursor, highlighting the importance of further research into the detection of these chemicals and elucidation of their eventual fates (Liu & Mejia Avendaño, 2013). The complexity of this class of chemicals makes effective monitoring difficult, but the general pattern is that wherever scientists search for PFAS, they find them.

While PFAS contamination is a global problem and the propensity for sorption or transport is specific to each chemical, the primary burden of PFAS pollution generally exists within local proximity to a specific point source (De Silva et al., 2021). Production facilities for fluorinated

compounds, wastewater treatment plants, use of firefighting foams, and agricultural application of PFAS are all significant sources of contamination (EEA, 2019).

While PFAS have not been produced in Denmark, they have been imported and utilized in a variety of industries. Lapses in regulation requiring transparency have allowed some industries to avoid reporting certain kinds of data regarding PFAS importation and utilization, making the quantity of total PFAS imported to Denmark unclear (Tvede & Frandsen, 2023). However, PFAS pollution within the Danish environment has been noted. When the Danish EPA evaluated PFAS levels in groundwater at contaminated sites within the country, they found the sum of 9 PFAS compounds to be around or above 1,000ng/l in four different sites (Larsen & Giovalle, 2015). For reference, the current limits on PFAS in Danish drinking water, based on the sum of PFOA, PFOS, PFNA, and PFHxS, is limited to 2ng/l (Rekik et al., 2024). The source of this pollution was firefighting foams in three of the four sites, and the pollution was attributed to the carpet industry in the fourth (Larsen & Giovalle, 2015). Given that groundwater is the source of Denmark's drinking water, remediation efforts and monitoring for these polluted sites and other locations with similar exposures have become a local priority.

The widespread nature of PFAS contamination throughout the global environment poses a risk for humans and wildlife alike, as it reaches into food chains, especially through seafood and polluted drinking water (Evich et al., 2022). PFAS have also been shown to translocate from the environment into plant tissues, primarily through diffusion into the roots, illustrating the pervasive nature of PFAS pollution once it has been released (Rekik et al., 2024). Controlling exposure once a pollutant already exists in the environment can be especially hard to manage. In contrast, exposure from consumer goods can be more effectively restricted via legislative routes, as Denmark has done by banning PFAS from food contact materials in 2020 (Danish Veterinary and Food Administration, 2020; Wang et al., 2017). However, with the already extensive spread of PFAS in the environment and the existence of contaminated sites internationally, the need for a remediation strategy is apparent.

1.5 Bioremediation of PFAS

A variety of conventional pollutant management strategies have been employed to face the challenge of remediating PFAS pollution. Techniques such as adsorption, filtration, thermal treatment, chemical oxidation and reduction reactions, and soil washing have all been used, each approach with its own advantages and disadvantages (Evich et al., 2022). The most common challenges of these treatment methods involve the necessity for *ex-situ* (off-site) treatment, high costs, intensive energy requirements, and the production of harmful waste products (Shahsavari et al., 2021). These challenges underscore the opportunity for a low-energy, *in situ* (on-site) remediation approach, which would be more cost-effective and less invasive to the polluted ecosystem (Y. Li et al., 2019).

Such a solution could consist of bioremediation, the technological utilization of a biological organism's ability to reduce pollutant loads through either metabolism or bioaccumulation. Plants, fungi, and bacteria can be used to degrade pollutants either through biologically catalyzed chemical reactions that alter the molecular structure of the contaminants or through the sequestering of pollutants within biomass, allowing for subsequent isolation or elimination methods. *In Situ* metabolic bioremediation efforts involve either inoculating a biological component into the site, as in bioaugmentation or managing the environmental conditions to better stimulate the native microbial community to perform detoxification, such as in biostimulation (Thacharodi et al., 2023). Such strategies have been successfully employed to degrade chlorinated solvents from contaminated groundwater (Xu et al., 2023). The first *in-situ* pilot-scale bioremediation of polychlorinated biphenyls (PCBs) was conducted in 2019, using *Dehalonium chlorocoercia* and *Paraburkholderia xenovorans* to reduce PCB concentration by 52% in sediments and 95% in porewater (Xu et al., 2023). Such biodegradation of organohalides tends to occur via reductive dehalogenation under anaerobic conditions, with many bacteria able to utilize the energy released by the reaction (Parsons et al., 2008). Analogous reductive defluorination has been hypothesized as a possible degradation pathway, but so far, this phenomenon has not been directly reported (M. Hu & Scott, 2024).

Bioremediation strategies for fluorinated compounds are still at the beginning of their development and face several significant hurdles, such as the strength of the carbon-fluorine bond, the newness of PFAS as a chemical class, and the toxicity of free fluoride to bacterial cells. However, the successful evolution of such biodegradation strategies for other

organohalides points to the possibility of developing an effective microbe-mediated PFAS degradation technique. Current research in this field aims to identify bacteria capable of breaking down PFAS compounds, understand associated degradation mechanisms and products, and map the genetic context regulating such activity.

1.5.1 Bacteria

Certain thermodynamic calculations suggest that the reductive defluorination of fluorinated compounds could provide enough energy to support the growth of organisms, but the kinetic stability of the carbon-fluorine (C-F) bond introduces a challenge that could explain the rarity of this phenomenon, in addition to limited availability of enzymes required to perform such a reaction in nature (Liu & Mejia Avendaño, 2013; Parsons et al., 2008). Seeing as PFAS are anthropogenic compounds and relatively new on the evolutionary timeline, the development of bacterial species to metabolize this species has had less time to develop. However, with biotechnological research advancements, this process could be expedited. In contrast, other studies have suggested that C-F bond reduction is not energetically favorable to bacteria as it cannot be coupled to a respiratory chain and generate ATP (Wackett, 2021). Cometabolic degradation of halogenated compounds by aerobic microorganisms has also been highlighted as a potentially significant degradation pathway. Biodegradation of mono-fluorinated aromatics has already been established, but PFAS biodegradation is still not fully understood (Kiel & Engesser, 2015). General degradation patterns see the functional groups of PFAS as a weak point in the chemical structure where degradation can begin. However, it is common that PFAS are not able to achieve complete mineralization and transformation products are often also fluorinated (Wackett, 2021).

An idealized fluorine degrader bacterial cell might contain passive uptake mechanisms for fluorinated compounds, any cofactor necessary for reductive dehalogenation, as well as a low-protentional ferredoxin reducing system, ATP, a sensor such as a fluoride riboswitch regulatory system, and the ability to synthesize an export pump that can remove the toxic fluoride from within the cell (Wackett, 2021). Isolating bacteria from PFAS-polluted areas could allow for optimal selection of microorganisms with the biological toolkit to perform degradation, as has been a successful strategy in finding remediating bacteria for hydrocarbon pollution (Shahsavari et al., 2021). At this stage of the research, a diverse range of bacteria have been studied under a variety of conditions. Table 1 shows a selection of PFAS degradation studies and summarizes

study conditions and results. Additional studies about PFAS degrading bacteria are elaborated on in Section 3.4.

Microorganism	Fluorinated compound	Conditions	Degradation Product	% Degradation	Mechanism	Notes	Source
Acidimicrobium sp. strain A6 and AC enrichment culture	0.1 mg/L PFOS and 100mg/L PFOA	Anaerobic, 100 day incubation, low pH and iron rich environment	F− and flourinated intermediates: (HFBA), (PFPeA) (PFHxA) (PFHpA), acetate	33-50% -PFOA 63% -PFOA	A6 can defluorinate PFOA/PFOS while reducing iron, using ammonium or hydrogen as the electron donor.	A6 is known for Feammox rxns. Enrichment culture was more effective than pure culture. DOC goes down over time for enrichment culture.	Huang & Jaffé, 2019
Pseudomonas PS27 and PDMF10 isolated from PFAs contaminated soil	PFHxS	Alkanotrophic. Incubated at 27 ◦C with shaking (150 rpm) under microaerophilic conditions for 3 weeks. Ethanol-octane or octane as growth substrate	Bioaccumulated	32 ± 1% removal by ethanol-octane grown PS27 and 28 ± 1% removal by octane-adapted PDMF10). 40% ± 3% removal with both isolates as mixed culture.	Co-metabolism	Morphological changes in exposed cells	Presentato et al., 2020
Community of microorganisms from soil	8-2 fluorotelomer alcohol	Soil and headspace, incubated for 7 months. Aerobic. Static and continuous headspace flow	8-2 FTUA 2H-PFOA 7-3 FTUA 3-OH-7-3 Acid 7-3 Acid (11%) 7-2 sFTOH PFOA (25% of yield) PFHxA (4%)	100% for 8-2 FTOH lost but there was some soil adsorption and breakdown into other fluorinated compounds	Unknown		Wang et al., 2009
Cell extracts from *Thauera aromatica*	2-F-benzoate	Cells extracts were taken from the anaerobic denitrifying strain *T. aromatica* grown with 2-F-benzoate and benzoate as sole carbon sources and nitrate as an electron acceptor	CO2 and HF	100%	Activation of 2-F-benzoate by a AMP- forming benzoate-CoA ligase, the 2-F-BzCoA is dearomatized by BCR to a mixture of 2-F- and 6-F-cyclohexa-1,5-diene-1-carboxyl-CoA (2-F-/6-F- 1,5-dienoyl-CoA). Defluorination by enoyl-CoA hydratases/hydrolases.		Tiedt et al., 2017
Gordonia sp. strain NB4-1Y	6:2 fluorotelomer sulfonamidoalkyl betaine and 6:2 fluorotelomer sulfonate	Sulfur-limited conditions. 168 hour incubation.	PFBA, PFPeA, PFHxA, perfluoroheptanoic acid (PFHpA), 4:3 FTCA, 5:3 FTCA, 6:2 FTCA, 6:2 FTUA, 5:2 sFTOH, 5:2 FT ketone, and 6:2 FTOH	9.9% of 6:2 FTSA and 70.4% of 6:2 FTAB	6:2 FTSA to 6:2 FTAL is biologically mediated by two nitrilotriacetate monooxygenases, conversion of 6:2 FTCA to 6:2 FTUCA is chemically-mediated through the spontaneous loss of hydrogen fluoride		Bottos et al., 2020
Mixed bacterial culture (90 d) and aerobic soil (180 d).	6-2 fluorotelomer alcohol	Mixed aerobic bacterial culture from activated sludge exposed to fluorinated chemicals	Mixed culture: 6-2 FTA (6%), 6-2 FTUA (23%), 5-2 sFTOH (16%), 5-3 acid (6%),PFHxA (5%) Soil: PFPeA (30%), PFHxA (8%), , PFBA (2%), 5-3 acid (15%) Net fluoride increase was 15.8 nmol/mL equivalent to 16% of total 6-2 FTOH mineralization	Unknown	6-2 FTOH is first oxidized to 6-2 fluorotelomer aldehyde (6-2 FTAL) catalyzed by alcohol dehydrogenase, then to 6-2 FTA catalyzed by aldehyde dehydrogenase. 6-2 FTUA degradation has two pathways. The formation of PFPeA and PFHxA is the dominant route, where 6-2 FTUA is converted to 5-2 FT ketone, then degrades to PFPeA (loss of two carbons) and PFHxA (loss of one carbon). The other pathway is unknown.	FBA, PFPeA, and 4-3 acid indicates that multiple –CF2– groups in 6-2 FTOH were removed	Liu & Mejia Avendaño, 2013
Rhodococcus sp. 065240	benzotrifluoride (BTF	*Rhodococcus* sp. cells grown at 28 °C for 48 h was inoculated at 1% into culture medium, after 24–72 h, 20 mM BTF was added to the culture, and cultivation continued for 24–192 h. Aerobic conditions.	Unknown but detection of fluoride.	2.5%	Btf gene cluster related to dioxygenase pathway	Gene cluster likely reached this *Rhodococcus* via interspecies gene transfer	Yano et al., 2015

Table 1: Selected studies about PFAS degradation (Bottos et al., 2020b; Huang & Jaffé, 2019; Liu et al., 2010; Presentato et al., 2020; Tiedt et al., 2017; N. Wang et al., 2009; Yano et al., 2015).

1.5.2 Enzymes

The most well-documented microbial defluorination reaction occurs with one of the few naturally occurring organofluorine compounds, fluoroacetate. Fluoroacetate dehalogenase (FAc-DEX H1) is an enzyme produced by bacteria such as *Pseudomonas* and *Delftia acidovorans* that can catalyze the hydrolytic defluorination of fluoroacetate, yielding a fluoride ion and glycolate as the transformation product (M. Hu & Scott, 2024; Kurihara et al., 2003). When genetically modified *Butyrivibrio fibrisovens* rumen bacteria with the gene coding for fluoroacetate dehalogenase were introduced to sheep, the animals developed improved resistance to fluoroacetate poisoning (Donnelly & Murphy, 2009). The biotechnological applications of this enzyme have also been investigated when it comes to PFAS degradation. One study showed that fluoroacetate dehalogenase expressed in *E. Coli* BL21 catalyzed the defluorination of 2,3,3,3-tetrafluoropropionic acid (Y. Li et al., 2019). Other enzymes of interest when it comes to defluorination include haloacid dehalogenases, reductive dehalogenases, dioxygenases and monooxygenases, cytochrome P450, peroxides, laccaes, desulfonases, and mettalloenzymes (M. Hu & Scott, 2024; Wackett, 2021; Xu et al., 2023). Engineering of defluorination enzymes has also been considered. One study showed effective C-F bond cleavage by an engineered cysteine dioxygenase (Seong et al., 2019). Table 2 shows the most well-recognized enzymes associated with defluorination and the potential chemical reactions they are able to catalyze. Table 3 shows the specific enzymes of interest utilized in this study and explains their relevance in regard to defluorination.

Enzymes	Reactions
Haloacid dehalogenases	**F**-CH_2-COOH + H_2O → **OH**-R-CH_2-COOH + H^+ + F^-
Reductive dehalogenases[a]	**F**-R-CH_2-COOH + $2e^-$ + H^+ → **H**-R-CH_2-COOH + F^-
Cytochromes P450, monooxygenases[a]	**F**-C-R + O_2 + $2e^-$ + $2H^+$ + NAD(P)H → **OH**-C-R + $NAD(P)^+$ + H_2O + H^+ + F^-
Peroxidases[a]	**2** F-C-R + med + H_2O_2 → **F**-C-R + $2med^-$ + $2H_2O$ → 2med-C-R + $2F^-$ + $2H_2O$
Laccases[a]	**4** F-C-R + $4e^-$ + 4med + O_2 → **F**-C-R + $4med^-$ + $2H_2O$ → 4med-C-R + $4F^-$ + $2H_2O$
Desulfonases[a]	**F**-R-CH_2-SO_3H + FMN + NAD(P)H + H^+ → **F**-R-CHO + FMN + $NAD(P)^+$ + H^+ + SO_3^{2-}

Table 2: Enzymes related to defluorination and their associated chemical reactions as shown in Toward the Development of a Molecular Toolkit for the Microbial Remediation of Per-and polyfluoroalkyl Substances (M. Hu & Scott, 2024).

Enzyme	Gene ID	Bacteria	More info	Source
Fluoroacetate dehalogenase	FAc-DEX FA1 BAE94252.1	*Burkholderia* sp. FA1	Catalyzes the hydrolytic defluorination of fluoroacetate to produce glycolate and fluoride	Kurihara et al., 2003
Toluene dioxygenase	WP_012052601	*Pseudomonas putida* F1	Made of: flavoprotein reductase (TodA), a ferredoxin (TodB), and the Rieske dioxygenase protein (TodC1C2). Substrate specificity determined by toluene dioxygenase	Bygd et al., 2021
1.Alcohol dehydrogenases 2.Luciferase-like monooxygenase (LLM) class flavin-dependent oxidoreductase genes	1.RS16300 RS02605 RS18475 RS08865 2.RS22855 RS00415 RS1416, RS10415 RS14165 RS14725	*Gordonia* sp. strain NB4-1Y	These genes were overexpressed in 6:2 FTAB and 6:2 FTSA cultures.	Bottos et al., 2020
Haloacid dehalogenases: DeHa type I DeHa type II	PZP66635.1 WP_011137954.1	*Delftia acidovorans*	Cloned this gene in *E.Coli* and saw F-	Harris et al., 2022
Upregulate: class I BzCoA reductase (BCR) Downregulate: benzoate- CoA ligase (BCL)	*bcrABCD:* AAX84174.1 AAX84166.1 AAX84119.1 *bcl* WP_107220371.1	*Thauera aromatica* **anaerobic*	Mechansim: Birch reduction-like mechanism resulting in a formal nucleophilic aromatic substitution	Tiedt et al., 2017
btf gene cluster, highly homologous to the ipb gene cluster of R. erythropolis BD2. The btf gene cluster contains all genes corresponding to the ipbA1, ipbA2, ipbA3, ipbA4, ipbB, ipbC, and ipbD, in addition to the ipbS and ipbT, encoding the two-component system IpbST, which control the expression of the ipb genes	ipbA1: AAP74038.1 ipbA2: AAP74039.1 ipbA3: AAP74040.1 ipbA4:AAP74041.1 ipbB:AAP74043.1 ipbC: AAP74042.1 ipbD:AAP74059.1 ipbS:AAP74044.1 ipbT:AAP74045.1	*Rhodococcus* sp. 065240,	Dioxygenase pathway	Yano et al., 2015
L-2-haloacid dehalogenases	Adeh3811 Bpro0530 Bpro4516 RHA1_ro00230	Found in diverse bacteria	Novel enzymes found to hydrolyze fluoroacetate	Chan et al., 2011
One putative *hkd* gene encoding a haloalkane dehalogenase, five genes encoding P450-type monooxygenases (CYP), and three *alkB* genes encoding alkane monooxygenases	Hkd:*had*-2 (2814128232) CYP: 2814125567, 2814127004, 2814127041, 2814127155, 2814127435 alkB: *alkB*-1, *alkB*-2, and *alkB*-3	*Pseudomonas* sp. strain 273	Proposed as related to fluoroalkane metabolism	Xie et al., 2023

Table 3: Enzymes related to PFAS degradation and their associated genes (Bottos et al., 2020; Bygd et al., 2021; Chan et al., 2011; Harris et al., 2022; Kurihara et al., 2003; Tiedt et al., 2017; Xie et al., 2023; Yano et al., 2015).

1.5.3 Genetics

Understanding the genes encoding for enzymes involved in defluorination is a critical step to targeting PFAS degradation within microorganisms. Genetic markers associated with defluorination have been identified in several studies. One study found that a 2-keto-4-hydroxyglutarate aldolase gene and a gene coding for fluorothreonyl-tRNA deacylase were linked to bacterial defluorination and subsequent resistance to the naturally occurring antibiotic 4-fluorothreonine (Wu & Deng, 2020). Another study found that several genes encoding reductive dehalogenases, including a novel *rdhA* gene, were strongly correlated with fluoride production resulting from PFOS and PFOA degradation by the *Acidimicrobium* sp. Strain A6, which was capable of degrading up to 60% of PFOS and PFOA while producing fluoride and shorter chain PFAAs as transformation products (Huang & Jaffé, 2019; Jaffé et al., 2024). A gene knockout experiment lent additional support to the significance of these genes in defluorination (Huang & Jaffé, 2019). One transcriptomic study looked at *Gordonia* sp. NB4-1Y, which degrades the sulfonated components of fluorotelemors like 6:2 fluorotelemor sulfonic acid (6:2 FTSA) and 6:2 fluorotelemor sulfonamide alkylbetaine (6:2 FTAB) under sulfur-limited conditions, creating perfluorinated carboxylic acids as the end product along with other shorter chain transformation products (Bottos et al., 2020). The study showed a shift in gene expression related to this degradation activity that involved altered expression of genes associated with sulfur transport and dehydrogenases, oxygenases, oxidoreductases, acetyl-CoA transferases, and carbon-nitrogen bond cleavage (Bottos et al., 2020).

Such altered genetic expression linked to degradation shows the importance of gene regulation in pollution resistance and degradation activity in bacteria and provides insight into the potential mechanisms responsible for such abilities. It has been hypothesized that mobile genetic elements with strong gene promoters may have an association with overexpression of degradation genes, which could confer bacteria's degradative abilities.

1.6 Project Objective

The work for this thesis involved screening for PFAS degradation activity from microbes in environmental samples collected from contaminated sites in Denmark. The sampling campaign was conducted on-site. The microbial laboratory experiments were done in the Microbial Ecology and Biotechnology (MEB) section at the University of Copenhagen. The chemical analysis was conducted by Martin Hansen at Aarhus University in Roskilde in the Environmental Chemistry and Toxicology (MITO) section.

The work for this thesis can be divided into the following sections.

1. Sampling of soil and water from contaminated sites
2. Positive Control Defluorination Experiment
3. 96-well Colorimetric Assay
    a. Method development
    b. Screening
4. DNA Extraction and Nanopore Sequencing
5. Chemical Analysis

Soil and water samples were collected from sites with a history of PFAS pollution with the objective of finding microbes that were more likely to have developed a tolerance or degradation mechanism for these compounds. A previous defluorination study was replicated using *P. putida* F1, which can break down the fluorinated compound DFBD. This preliminary experiment reiterated the ability of some bacteria to break C-F bonds under certain conditions and served as a positive control for the subsequent development of methods for a 96-well colorimetric assay, which can signal degradation of PFAS through color change resulting from the presence of free fluoride. This assay was used to screen dilutions of bacteria from the environmental samples for indications of PFOA degradation. Colorimetric assay results indicative of defluorination were followed by DNA extraction and nanopore sequencing of the sample of interest. Analysis was conducted to determine the bacterial species in the samples, and a search for genes previously identified as coding for enzymes related to defluorination was conducted. Lastly, samples were analyzed using analytical chemistry techniques to verify PFOA degradation and identify any degradation products. A general workflow of the project is included in Figure 3.

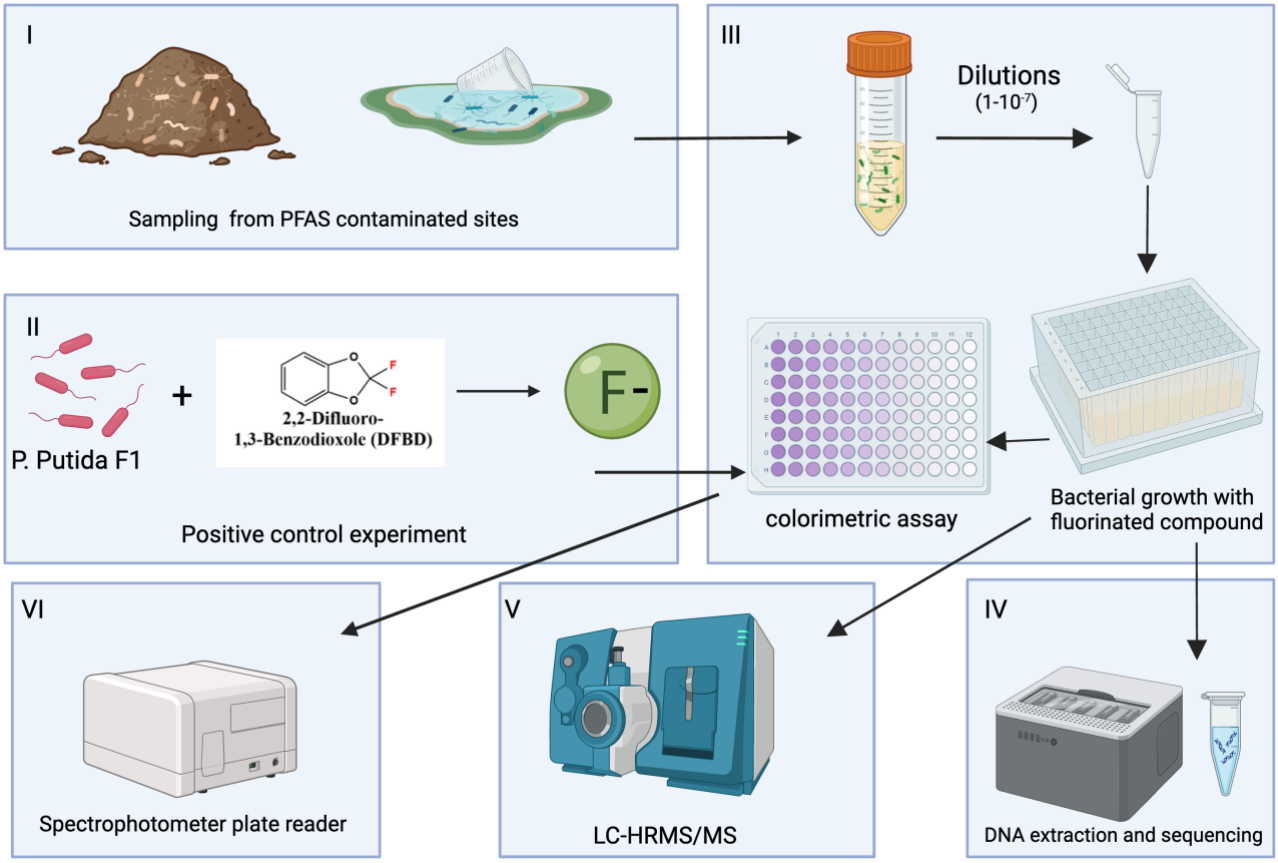

Figure 3: Visual overview of activities for this thesis. Created with BioRender.com

2. Materials and Methods

2.1 Sampling of Soil and Water from Contaminated Sites

2.1.1 Objective

Soil and water samples were collected from two contaminated sites in Denmark as a source of microbes with potential PFAS degradation abilities. Both locations are contaminated with PFAS due to the use of Aqueous Film Forming Foams (AFFFs) for firefighting training and related activities. Site 1 is undisclosed in this thesis. Site 2 is currently Denmark's first PFAS testing center, the result of a collaborative effort between Rednings Og Sikkerhedcenter (RESC), an operational fire academy located on the premises, the Slagelse Municipality, which owns the land and acts as the local environmental authority, and Region Sjælland, which is the environmental authority for the entire region (Region Sjælland, 2023).

2.1.2 Methods

Site 1:

Water: Groundwater samples were collected on February 26, 2024, which were selected based on previous PFAS measurements. Samples were extracted from the depths that showed the highest PFAS concentrations for each borehole.

Soil: Soil samples from top layer soil (10-20cm), roots from the topsoil (10 cm deep), middle zone soil (10cm-20cm), and clay subsoil (20cm-30cm) were collected on a later date from this site by Tue Kjærgaard Nielsen and used in this project.

Site 2:

Water: Samples were collected on February 22, 2024, from three different sites in the area: Gangro Beach, Korsør Nor, and the Korsør test center. These sites were chosen based on measurements taken in 2021 by the test center, which documented PFOS content of up to .42 µg/l in groundwater at the test center (Region Slagelse Kommune, 2021). The water collected from the test center was groundwater, while the water samples from Gangro Beach and Korsør Nor were surface water.

Soil: Soil samples were also collected on February 22, 2024, from the same three sites in the area: Gangro Beach, Korsør Nor, and the Korsør PFAS test center. At Gangro Beach, two samples of sandy soil were collected. At Korsør Nor, one sample of sandy soil and one sample of topsoil was collected. At the Korsør test center, one sample of clay subsoil and one sample of topsoil was collected. The selection of these locations was informed by 2021 measurements, which showed PFOS content as high as 120µg/kg near the Korsør test center and measurements of 68.2µg/kg PFOS near Korsør Nor (Region Slagelse Kommune, 2021).

All soil and water samples from both sites were stored in the 4°C storage refrigerator at PLEN at the University of Copenhagen.

2.2 Positive Control Defluorination Experiment

2.2.1 Objective

The goal of this experiment was to replicate a previously published experiment by Bygd et al., published in 2021, which demonstrated fluoride release through the degradation of 2,2-difluoro-1,3-benzodioxole (DFBD) by *P. putida* F1 induced with toluene. Within the context of this project, this experiment served as a positive control and initial test to ensure the effectiveness of the subsequent colorimetric assays.

2.2.2 Methods

Pseudomonas alloputida F1 (DSM 6899) was ordered as a freeze-dried culture product from DSMZ Webshop and rehydrated before cultivation on Luria-Bertani (LB) plates. An overnight culture was prepared by inoculating a single colony into M9 media with either toluene as the sole carbon source or toluene with 20% glucose. After 24 hours of incubation with shaking at 28°C, the overnight culture was exposed to DFBD, and additional M9 media was added. Samples were pelleted, and 1mL of supernatant was extracted at time points ranging from 30min to 24 hours. These samples were combined with 1mL of Total Ionic Strength Adjustment Buffer II (TISAB II) in a 5mL falcon tube, and fluoride concentrations were recorded using an Orion Dual Star pH/ISE meter and electrode. Before use, the Orion Dual Star pH/ISE meter and electrode were calibrated using standards with known fluoride concentrations of .5 ppm, 2 ppm, 10 ppm, and 20 ppm (Thermo Scientific, 2015).

2.2.3 Protocol Optimization

Various parameters were adjusted to optimize the experimental protocol and see successful defluorination. Experiments included adjusting the method of DFBD exposure. This consisted of using an upside-down flask in a bottle and a test tube in a bottle to create a system similar to a vapor bulb, wherein toluene and DFBD exposure occur gradually through evaporation. Alternatively, the chemicals were added in liquid form directly to the media. Additionally, the presence of glucose in the media was tested and compared to the use of toluene alone. Two media were tested, both were M9 media, but they were prepared on different days. All samples received 500µM DFBD in addition to the conditions described below.

Sample 1: Test tube, toluene, media one
Sample 2: Flask, toluene, media one
Sample 3: Test tube, glucose, media one
Sample 4: Flask, glucose, media one
Sample 5: Test tube, glucose, media two
Sample 6: Flask, glucose, media two
Sample 7: Test tube, toluene, media two
Sample 8: Flask, toluene, media two

The experiment was repeated with DFBD and toluene added directly to the media, rather than through the flask or test tube exposure method. In the subsequent experiment, toluene was used as the sole carbon source. Additionally, two different antibiotics, kanamycin and tetracycline, were also tested at concentrations of 10µg/mL and 20µg/mL.

2.2.4 Optimized Protocol Methods

An overnight culture was prepared by inoculating a single colony into 10 mL of M9 media. 10 µL of toluene was added directly to the media. After 24 hours of incubation with shaking at 28°C, 6 µL DFBD was added directly to the media. Samples were pelleted, and 1 mL of supernatant was extracted at time points 30 min, 2 hours, 4 hours, 6 hours, and 24 hours and added to 1mL of Total Ionic Strength Adjustment Buffer II (TISAB II) in a 5mL falcon tube. Fluoride concentrations were recorded using an Orion Dual Star pH/ISE meter and electrode.

Three samples were included, all with the same treatment. Three controls were also included: one without bacteria, one without DFBD, and one without toluene.

2.3 Colorimetric Assay – Method Development

2.3.1 Objective

The 96-well colorimetric assay used in this thesis was originally proposed for the degradation screening of fluorinated compounds by Bygd et al. in 2022. The assay uses a lanthanum-alizarin complex that binds to fluoride, changing to a purple color as a signal of defluorination (Bygd et al., 2022). With the aim of developing a protocol that effectively saw this color change due to the presence of fluoride, methods were initially developed using *P. putida* F1 induced with toluene and incubated with DFBD. This functioned as a positive control. The resulting fluoride from this defluorination reaction was quantified using an ion-selective electrode in parallel to monitoring color change, which served to validate the effectiveness of the colorimetric assay.

2.3.2 Bacterial Growth

P. putida F1 was cultured in 50 mL falcon tubes containing 10 mL of M9 media with 5µL of toluene as the sole carbon source by inoculation with a single colony. Following a 24-hour incubation period, cultures were pelleted, the supernatant was removed, and cells were resuspended in 5 mL of 20 mM HEPES buffer. 500 µL of DFBD was added at concentrations of 80 mM, 70 mM, 60 mM, and 40 mM. The cultures were then incubated overnight at 28°C with shaking at 200 rpm. Samples were then centrifuged, and 1mL of supernatant was extracted and added to 1mL TISAB II for fluoride measurement using a Thermo Scientific Orion Dual Star Ion Selective Electrode. Additional supernatant was used to assess color change via the chemical reaction described below.

2.3.3 Chemical Reaction

In either a cuvette or a 96-microwell plate, reagents were added consistent with the order and ratios described in the original paper (Bygd et al., 2022). Alizarin comprised 10% of the final volume, acetate buffer was 5%, lanthanum at 10%, samples containing fluoride made up 50%, and acetone comprised 25% of the final volume. Initial experiments used conditions specified in the previous paper, 50µM alizarin and lanthanum, along with the acetate buffer around pH 5. However, upon experimentation, we found that the methodology described in another paper was more effective, so the molarity of alizarin and lanthanum was increased to 500µM each, and the molarity of the acetate buffer was increased from 84mM to 1.68M as described in Khan et al., 2023.

2.3.4 Spectrophotometer

A V-1200 Spectrophotometer was used to take readings from the samples prepared in cuvettes. A BioTek® Epoch Microplate Spectrophotometer was used to take spectrophotometer readings from the samples prepared in microwell plates. Measurements of all samples were taken at both 530 nm and 620 nm.

2.3.5 Chemicals

Alizarin-3-methyliminodiacetic acid and Lanthanum (III) nitrate hexahydrate were from Sigma-Aldrich. Alizarin and lanthanum solutions were all prepared to concentrations of 500µM with 20 mM HEPES as the solvent. Acetate buffer was prepared at 1.68M using sodium acetate and glacial acid in distilled H_2O at a pH of 4.8. 2,2-difluoro-1,3-benzodioxole (DFBD) was produced by Aldrich Chemistry at 97% purity. Perfluorooctanoic acid (PFOA) was from Sigma Aldrich at 96% purity and was prepared to 40mM concentration in 20mM HEPES.

2.4 Colorimetric Assay – Screening

2.4.1 Objective

The 96-well colorimetric assay was utilized as a high throughput method for screening bacterial dilutions from environmental samples for microbial defluorination activity of PFOA.

2.4.2 Bacterial Growth

Dilutions of bacteria from soil samples collected at polluted sites were prepared by vortexing 5 grams of soil with 10 mL of either Phosphate Buffered Saline (PBS) or 20 mM HEPES in a 50 mL falcon tube. This initial concentration served as the first sample, followed by further serial dilutions using MilliQ water for samples prepared with HEPES and additional PBS for those with PBS, up to 10^{-7}. The dilutions of bacteria from the environmental samples were then added to a 96-well deep well plate in either 100µL or 50µL quantities, along with LB (Luria-Bertani) broth (with or without 1µl toluene/well) or M9 media (with toluene, MCPA, or glucose as the carbon source) in either 900µL or 450µL quantities respectively. 100µL of 40 mM PFOA was also added to the wells. Plates were placed in a 28°C incubator on a shaker at 200 rpm for 48 hours. After 48 hours, the plates were pelleted for 15 minutes at 2,700 rcf at 20°C with a swinging bucket rotor. The supernatant was removed, the cells were resuspended with 20 mM HEPES, and 100µL of 40 mM PFOA was added. The plates were then incubated for 48 hours at 28°C on a shaker at 200 rpm. Plates were pelleted in the same manner as before, then 100µL of supernatant was removed and used for testing as described in the chemical reaction section.

2.4.3 Chemical Reaction

A new flat-bottom 96-well plate was prepared for colorimetric analysis by adding 20µL of 500mM Alizarin-3-methyliminodiacetic acid, 10µL of acetate buffer (1.6M and pH 7), and 20µL of 500mM Lanthanum (III) nitrate hexahydrate to each of the wells, in that order. 100µL of the final supernatant from the bacterial growth procedure was added, followed by 50µL of acetone.

2.4.4 Controls

Positive controls received the same treatment as samples, but the supernatant was instead extracted from *P. putida* F1 grown with toluene and exposed to varying concentrations of DFBD (50 mM-80 mM). These samples had been previously tested with an Orion Dual Star pH/ISE meter and electrode and been shown to contain fluoride. Negative controls received the same treatment as samples for the chemical reaction, but instead of the addition of the supernatant, HEPES or MilliQ water was added.

The spectrophotometer and chemical information are the same as in Section 2.4.4 and Section 2.4.5.

2.5 DNA Extraction and Sequencing

2.5.1 Objective

DNA extraction and nanopore sequencing were performed on samples from wells displaying color change during the screening assay, to identify the bacteria present in the environmental samples and acquire genomic data that could be used to look for gene sequences homologous to those identified in previous studies as being related to defluorination activity.

2.5.2 DNA Extraction

DNA extractions were conducted using the Bead-Beat Micro AX Gravity kit by A&A Biotechnology following the manufacturer's protocol. Two days after the chemical screening portion of the assay, 100µL samples were taken for DNA extraction from the original 96-deep well plate, which had been stored in the refrigerator at 4°C after the bacterial cells were resuspended in the existing HEPES solution. These 100µL samples were centrifuged, and the supernatant was discarded. Lysis buffer and proteinase K were added, and then samples were bead-beaten for 40 seconds at 6.0m/sec using a FasrPrep-24TM 5G by MP Biomedicals. Samples were incubated for 30 min in an Eppendorf Thermomixer at 50°C at 1400rpm. RNA digestion was performed. Micro AXD columns and gravity tubes were prepared and equilibrated. Samples were then centrifuged at 12000rpm, and supernatant was applied to columns and then washed with two wash solutions. A small amount of E elution buffer was applied to reduce the final elute volume. A neutralizing buffer was applied to the bottom of the elution tubes, and then 120µL of E elution buffer was applied to release the DNA from the column. Eluted DNA was stored at 4°C.

2.5.3 DNA Concentration

DNA was concentrated using a DNA Clean & Concentrator™-5 kit by Zymo Research according to the manufacturer's protocol. In summary, DNA Binding Buffer was applied in a 2:1 ratio to each sample. The mixture was transferred to a Zymo-Spin™ Column in a Collection Tube and centrifuged for 30 seconds at 12,000rcf, and the flow through was discarded. The column was washed twice, and then the DNA was eluted in a final volume of 6µL.

2.5.4 DNA Quantification and Qualification

The quantity and quality of DNA extraction were assessed using an Invitrogen Qubit® 2.0 fluorometer and the Qubit 1X dsDNA High Sensitivity Assay Kit, which combined 198µL of Quibit working solution with 2µL from our sample and used two standards included in the kit. A NanoDrop ND-1000 Spectrophotometer was used to assess DNA concentration by first calibrating with a water blank and then measuring 1.5µL of the sample.

2.5.5 Nanopore Sequencing

The nanopore sequencing was completed with the help of Tue K. Nielsen. DNA was prepared for sequencing using the Rapid Barcoding Kit SQK-RBK114.24 according to the manufacturer's protocol. The prepared DNA libraries were loaded onto an Oxford Nanopore MinION sequencer with an R10.4.1 flow cell. The sequencer was run according to manufacturer instructions. Reads were assembled by Tue K. Nielsen.

2.6 Chemical Analysis

2.6.1 Objective

To determine whether PFOA degradation had taken place in the samples of interest as indicated by the colorimetric assay, more precise chemical analysis methods were utilized to assess PFOA quantity and look for relevant transformation products.

2.6.2 Sample Preparation

100µL of the supernatant from the bacterial growth section of the colorimetric assay was preserved in an Eppendorf tube at 4°C. Samples were chosen for analysis based on the results of the colorimetric assay. Additionally, a positive control with the same amount of HEPES and PFOA but no bacterial exposure was prepared, in addition to a plastic control, which consisted of HEPES in an Eppendorf tube.

2.6.3 Chemical Analysis

The following chemical analysis was performed by Martin Hansen at Aarhus University in Roskilde in the Environmental Chemistry and Toxicology (Miljøkemi og Toksikologi, MITO) section.

All samples were diluted 100,000 times, fortified with isotopically labeled PFAS standards, and analyzed using liquid chromatography high-resolution tandem mass spectrometry (LC-HRMS/MS). A Dionex Ultimate 3000 RSLCnano system coupled to a ThermoFisher Scientific Q Exactive HF high-resolution accurate-mass Orbitrap mass spectrometer was used. Using a Wellington reference mixture of 29 different PFAS (including PFBA, PFPeA, PFHxA, PFHpA, PFOA) analytes were separated using a C18, 100 Å, 2 µm, 150 mm × 50 µm, column kept at 40^{o}C. A biphasic gradient delivered at 500 nL/min with water, methanol and isopropanol was applied to elute the PFAS with an injection volume of 1 µL. The HRMS system was operated in negative ESI mode in data-dependent acquisition mode (Top5) with a mass resolution of 240 000 and the scan range of 70 – 1050 m/z.

3. Results and Discussion

3.1 Positive Control Defluorination Experiment

3.1.1 Protocol Optimization Process

The Trial 1 experiment indicated successful defluorination of DFBD by *P. putida* F1 due to the detection of free fluoride in the supernatant as shown in Table 4. Higher concentrations of fluoride were detected after 24 hours of incubation as compared to 40 minutes. Consistent with the results in the previous study, color change occurred in the media with measured fluoride (Bygd et al., 2021a). The samples with a higher fluoride concentration saw more intense darkening of the media. In sample four, the presence of a dark, string-like precipitate was also noted, as shown in Figure 4. This substance is likely 1,2,3-trihydroxybenzene, also known as pyrogallol. The previous study found that DFBD could be oxidized by a toluene dioxygenase synthesized by *P. putida* F1 which catalyzes the degradation of DFBD into three short-lived intermediates that eventually end up as carbon dioxide, fluoride, and pyrogallol, which then oxidizes to a colored product responsible for the darkening of the medium (Bygd et al., 2021b).

The three highest fluoride measurements came from samples with different treatments. Sample four, which saw the highest concentration of free fluoride, did not receive toluene. This could indicate that induction with toluene is not necessary for *P. putida* to engage in defluorination activity. It is possible that the genes coding for the responsible toluene dioxygenase are constitutively expressed or that they are stimulated by the presence of DFBD. The other two samples with the highest fluoride measurements were samples five and seven, which were both treated with toluene, suggesting it also did not have an inhibitory effect. Sample five was grown in media with glucose and sample seven was grown in media without glucose, suggesting that the additional carbon source did not have a supplementary effect on DFBD degradation. Both samples were exposed to DFBD via test tube, during which the substance dripped directly into the media. The successful degradation that occurred in these samples showed that adding the chemicals directly to the media not only didn’t result in cell death but also may have heightened defluorination activity.

Based on these observations, the experimental design was refined. It was decided that DFBD and toluene would be directly added to the media. M9 media without additional glucose would be used, with toluene as the sole carbon source. This could exert extra selective pressure for the

expression of toluene dioxygenase genes while acting as a selective measure for *P. putida* F1 to safeguard against potential contamination.

Sample	F- ppm at 40 minutes	F- ppm at 24 hours
S1	.04	.9
S2	.05	.1
S3	.05	.1
S4	.05	4.2
S5	.06	2.1
S6	.05	.06
S7	.04	2.7
S8	.04	.05

Table 4: Fluoride measurements by ion selective electrode.

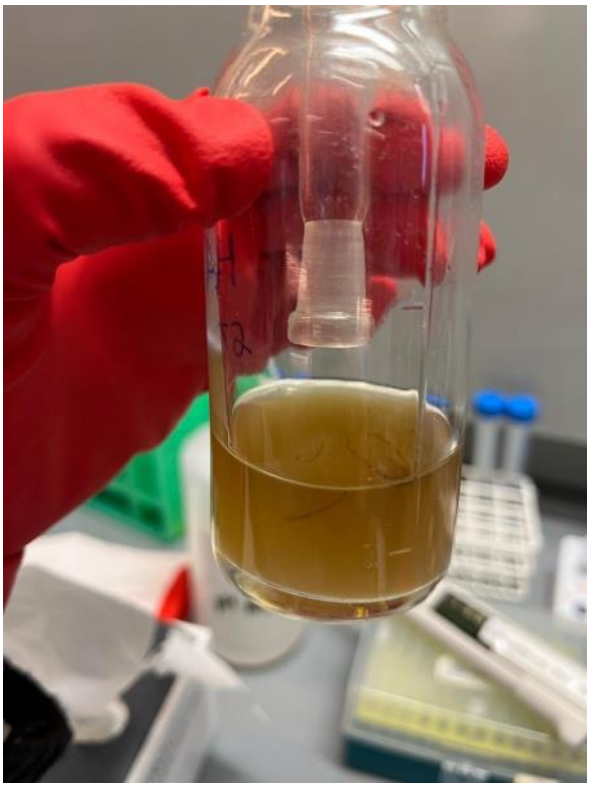

Figure 4: Image showing darkening of media and presence of substance likely to be pyrogallol

Preliminary results of the new experimental design were promising, with *P. putida* F1 using toluene as the sole carbon source and releasing 5.43 ppm of fluoride after just 4 hours of incubation, as shown in Table 5.

Sample Description	10 minutes	40 minutes	2 hours	4 hours
P. putida F1 + toluene + M9 w/glucose	.1	.3	.77	1.57
P. putida F1 + toluene + M9 w/out glucose	.5	1.5	3.7	5.43

Table 5: Fluoride (ppm) as measured by ion selective slectrode.

Antibiotics were investigated to select for *P. putida* F1 in our experimental setup, acting as an additional measure to mitigate the risk of contamination. The antibiotics tetracycline and kanamycin were selected as they had been used in previous studies with the same strain (Parales et al., 2013; Zylstra et al., 1988). Growth of *P. putida* F1 was tested with tetracycline and kanamycin at 10 and 20 µg/mL each, in 10 mL volumes of M9 media with glucose. Growth occurred in the culture with tetracycline, but at a slower rate than in the cultures without antibiotics. No growth occurred in the kanamycin samples. It was concluded that growth with toluene as the sole carbon source was effective enough as a selective measure for *P. putida* growth. Additionally, the fluoride detected in our samples likely indicates the presence of *P. putida* rather than contamination from another microorganism capable of defluorination.

3.1.2 Optimized Protocol Results and Discussion

The optimized protocol results support the findings that *P. putida* F1 induced with toluene is capable of breaking the C-F bond in DFBD, resulting in free fluoride, darkening of the media, and the presence of a degradation substance likely to be pyrogallol (Bygd et al., 2021). In our samples, the highest amount of fluoride was detected after 24 hours of incubation as shown in Table 6. This contrasts with the findings of Bygd et al., who saw fluoride concentrations stabilize after just 4 hours. Additionally, the concentrations of free fluoride released in this study varied compared to the previous study. While our experiment yielded a maximum of 9.8 ppm after 24 hours, the findings from the previous study saw a maximum fluoride concentration of 15.2 ppm after just 4 hours (Bygd et al., 2021). The difference between the two studies could be attributed to the use of different amounts of toluene or DFBD or the varying metabolic efficiency of the bacteria due to the experimental setup. Parameters such as oxygen availability or the timing of exposure within the bacterial lifecycle could have had an effect.

	30 minutes	2 hours	4 hours	6 hours	24 hours
S1	1.18	3.57	5.7	6.7	9.8
S2	1.1	3.1	5.1	6.0	8.5
S3	1.0	3.2	4.7	5.9	8.2
C1	0.0	0.0	0.0	0.0	0.0
C2	0.0	0.0	0.0	0.0	0.3
C3	0.0	0.0	0.0	0.0	0.0

Table 6: Fluoride concentration as detected by ion selective electrode in ppm.

Generally, the results of this experiment were sufficient to support the observation that *P. putida* F1 can degrade DFBD under the right conditions, seeing as free fluoride and darkening of the media were detected in all samples. Such transformation was not seen in the control without bacterial cells, showing that DFBD remains stable in the medium without bacterial intervention. Fluoride was not detected in samples that were never exposed to DFBD, suggesting that it is the source of the fluoride found in the medium. In control three, for the first 6 hours of incubation with *P. putida* F1 exposed to DFBD without prior toluene exposure, no degradation activity was observed. After 24 hours, a relatively small amount of fluoride was detected, .3 ppm. These results reiterate the importance of the toluene metabolic pathway, as the bacteria degrade DFBD much faster and more effectively when they have been exposed to toluene. This exposure functions to induce the synthesis of enzymes such as toluene dioxygenase which is composed of a flavoprotein reductase (TodA), a ferredoxin (TodB), and the Rieske dioxygenase protein ($TodC_1C_2$) and is proposed to be capable of oxidizing DFBD to cis-dihydrodiols which are likely unstable and undergo subsequent reactions resulting in defluorination (Bygd et al., 2021a).

Within the context of the larger project, the success of this experiment not only reiterated a relevant microbe-facilitated defluorination reaction but also set up the next stage of the research, as this well-documented defluorination reaction served as a positive control for the subsequent task of developing a protocol for the colorimetric screening assay.

3.2 Colorimetric Assay Method Development and Protocol Optimization

3.2.1 Objective

This goal of this experiment to development an effective protocol for the 96-well colorimetric described in the paper, Microwell Fluoride Screen for Chemical, Enzymatic, and Cellular Reactions Reveals Latent Microbial Defluorination Capacity for -CF_3 Groups published by Bygd et al, in 2022. The authors of this paper adapted a previous fluoride detection method that relies on the binding of fluoride ions to a complex formed by alizarin, which is known for its red color, and the rare earth metal lanthanum, as shown in Figure 5. They miniaturized this method to fit a microwell plate format and optimized the parameters for use in biological models.

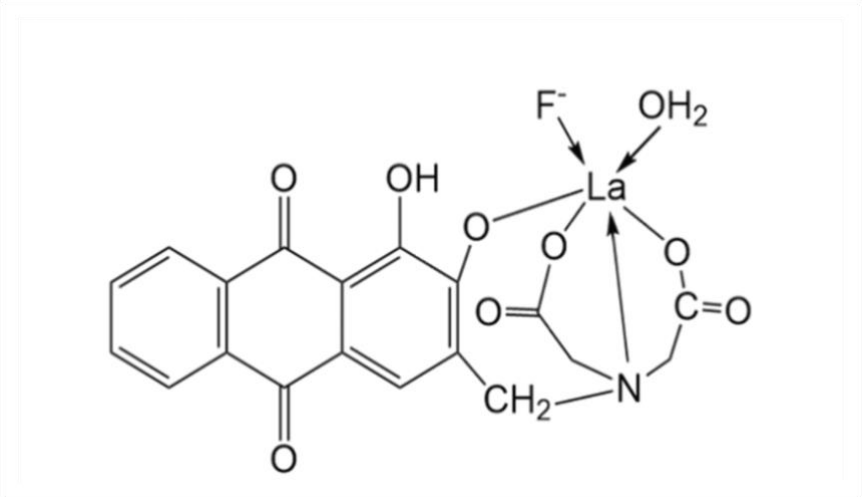

Figure 5: Lanthanum-alzarin complex bound to fluoride as shown in Microwell Fluoride Screen Chemical, Enzymatic, and Cellular Reactions Reveals Latent Microbial Defluorination Capacity for 2CF3 Groups (Bygd et al., 2022).

3.2.2 Trial 1

Utilizing the defluorination reaction described in the section 3.1, this trial successfully showed color change resulting from biological defluorination. A difference in color was observed between the pink shade of the alizarin-lanthanum complex unbound to fluoride and the purple shade of the samples with fluoride in the solution, as shown in Figure 6. Sample one had received DFBD AT 80µl, sample two at 70µL, sample three at 60µL and sample four at 50µM. Control one had received no DFBD and control two was water. Despite receiving treatment with different concentrations of DFBD, samples two, three, and four produced a similar shade of purple when observed visually. These results are consistent with the measured fluoride concentration as determined by ion ion-selective electrode which found that these samples were all within 1.5 ppm of each other, as shown in Table 7. Sample one stood out among the samples with the highest fluoride concentration of 13 ppm which also produced a noticeably darker purple, consistent with the observations in Bygd et al., which also noted darker purple colors associated with increased fluoride concentration (Bygd et al., 2022).

Sample	**Flouride Measurement (ppm)**
C1	0.00
S1	13.00
S2	8.23
S3	6.82
S4	6.89

Table 7: Fluoride concentration in ppm.

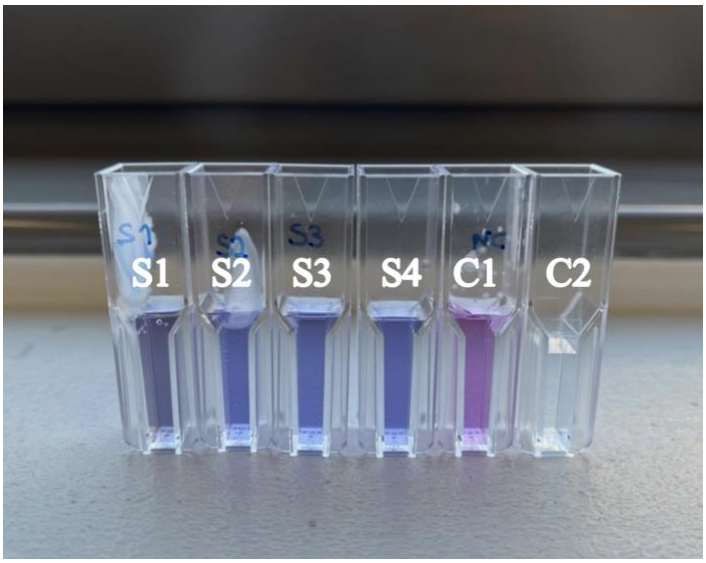

Figure 6: Image showing color change associated with fluoride binding to alazarin-lanthanum complex.

Spectrophotometer readings differed between the pink control with the unbound complex and the purple alizarin-lanthanum complex bound to fluoride. To quantify absorbance, the 620nm/530nm absorbance ratio was used based on the work of Bygd et al., who documented the UV-Vis spectra of the complex bound to water and fluoride. They found that 620nm was the peak absorbance of the fluoride-bound complex, while 530nm was the lambda maximum of the unbound complex (Bygd et al., 2022). The absorbance readings were taken at 2 minutes, then again at 15 minutes, with no significant difference found between these time points. Absorbance ratios were plotted against the amount of fluoride as detected by ion selective electrode in Figure 7. For both time points, sample one had the highest 620nm/530nm ratio, consistent with the results of the ion-selective electrode and the visual inspection for color change. However, the difference between this sample and the others in 620nm/530nm ratio was quite minimal. The sample one measurement at 2 min showed an absorbance ratio of 1.3, which was very close to the next highest respective ratio, which was sample four at 1.2. It is also notable that sample four had the a higher absorbance ratio than sample two, despite the higher amount of free fluoride in sample two as measured by the ion selective electrode.

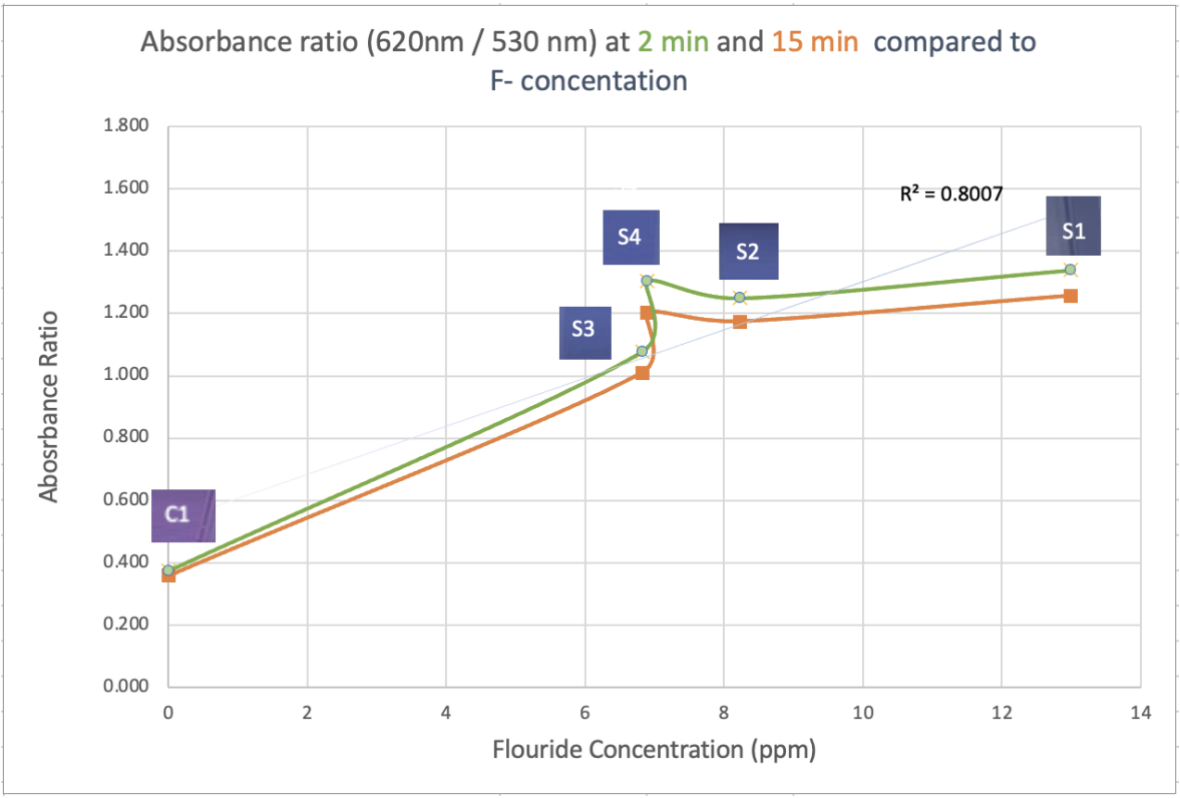

Figure 7: Absorbance ratio at 620nm/530nm compared to fluoride concentration as determined by ion selective electrode.

Overall, the absorbance ratios for all samples with free fluoride were quite similar to one another, within the range of 1-1.3. Despite the unexpected relationship within the samples, the difference between the samples with fluorine, and the control with no fluorine was significant. The unbound complex showed a 530nm/620nm ratio of around .4, which was the same found in the previous study (Bygd et al., 2022). This paper defined a “dark purple” well as having a 620nm/530nm ratio over .7, while a ‘light purple’ well was defined at .6, which was the cut-off point as defined for having detected fluoride in the system (Bygd et al., 2022). The high absorbance ratios found in this trial suggest that the amount of fluoride in the system may have been quite high, which could be the reason for the deviation from the expected trend exhibited in this trial. Alternatively, this phenomenon could be explained by the general similarity between the fluoride concentrations in the samples and small fluctuations in the measurement tools.

However, overall, the results of this trial were promising, showing a significant difference in the absorbance ratio between the control and the samples, as well as a clear color difference that could be observed visually to correlate with fluorine readings from the ion selective electrode.

3.2.3 Trial 2

A second trial was conducted, still using the defluorination reaction between *P. putida* F1 and DFBD, but this time in a microwell plate and with samples of lower fluoride concentration, to better determine the relationship between absorbance ratio and fluoride concentration.

The results of the second trial showed a strong linear relationship between fluoride concentration and absorbance ratio between 0 ppm and 2 ppm. These values plotted with the x-axis as the fluoride concentration and the absorbance ratio as the y-value and a linear fit, gives an R-squared value of .9. However, the linear model fits less well at concentrations above 2 ppm. The polynomial trendline with two orders better suits the entire data set, as shown in Figure 8. This trend could be explained by a limiting factor in the chemical reaction that produces the color change. The binding sites for the fluoride on the alizarin-lanthanum complex might become saturated, leading to a plateau in the color change at higher fluoride concentrations, which can also be seen visually as the different shades of purple become closer to one another at higher concentrations. The observed pattern was also noted in the paper originally describing the screening method, as it found fluoride concentration to be linearly related to absorbance ratio in the range of .19 ppm and 1.9 ppm (Bygd et al., 2022).

Second trial results indicated that the technique behind the colorimetric screening reliably produced color change in the presence of biologically mediated defluorination. It also gave a visual reference to see how the color produced by the complex relates to the amount of fluoride present. Lastly, it gave insight into the nature of the relationship between fluoride concentration and absorbance ratio, supporting the earlier observation that wells with a 620nm/530nm absorbance ratio over .7 are likely candidates to have fluoride in them (Bygd et al., 2022).

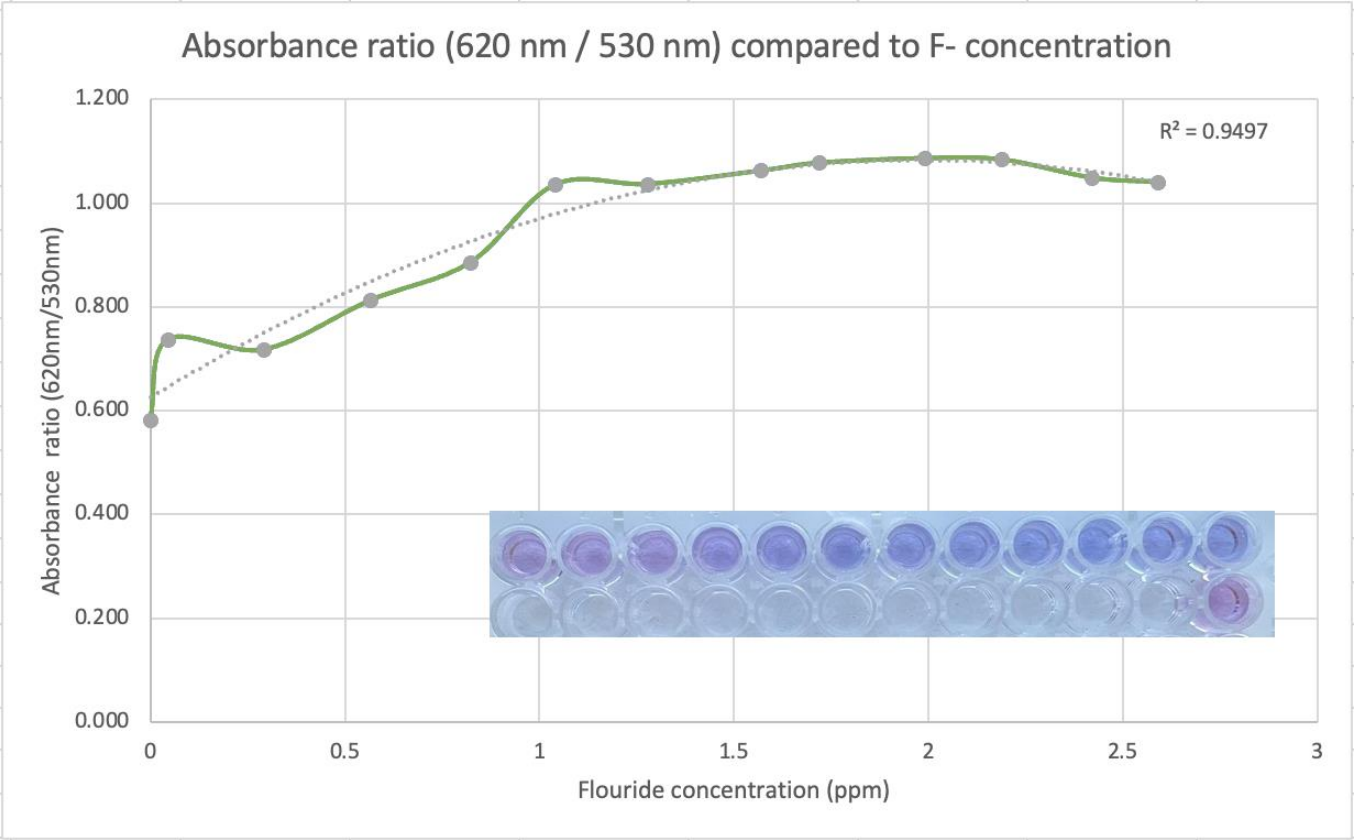

Figure 8: 620nm/530nm absorbance ratio of the samples compared to fluoride concentration in ppm as measured by ion-selective electrode. The cells are pictured with the 0 ppm control on the bottom right and the concentrations increasing from left to right in the top row.

3.3 Colorimetric Assay - Screening

3.3.1 Trial One

The initial bacterial screening using the colorimetric assay confirmed the protocol's effectiveness, with positive controls showing the expected darkening and purple color change, while the negative controls stayed pink, as shown in Figure 9. The most notable samples were found in wells F5 and G6. Sample F5 appeared visually darker than the other samples and controls, while G6 showed precipitated purple dye. This precipitation could be a signal of defluorination as a degradation product of PFOA may have reacted with one or more of the chemicals used in the colorimetric assay. Samples E5 and D7 were also of interest as they had a slightly darker color but were still fairly similar to the controls.

Measurements were taken using an ion-selective electrode to determine if fluoride was present in these wells. All readings were 0.00 ppm, suggesting either a lack of free fluoride or fluoride concentrations below the detection limit of the method. The Orion Dual Star pH/ISE meter was calibrated with fluoride concentrations of 0.5 ppm, 2 ppm, 10 ppm, and 20 ppm, which may be significantly higher than the fluoride levels in the samples. This could limit the electrode’s sensitivity to low fluoride concentrations, whereas the colorimetric assay can exhibit color change with just a few nanomoles of fluoride (Bygd et al., 2022). It is also possible that a defluorination reaction could be captured by the colorimetric assay due to its binding complex that rapidly reacts with free fluoride as it is released, in contrast with the electrode that may be unable to detect this fluoride because it has already reacted with another component in the media, forming a new product and therefore never accumulating to detectable levels.

This experiment provided additional evidence of the effectiveness of the protocol and showed promising preliminary signs of degradation activity of PFOA by the environmental bacteria. However, the absence of spectrophotometer data and any quantitative confirmation of defluorination were limitations.

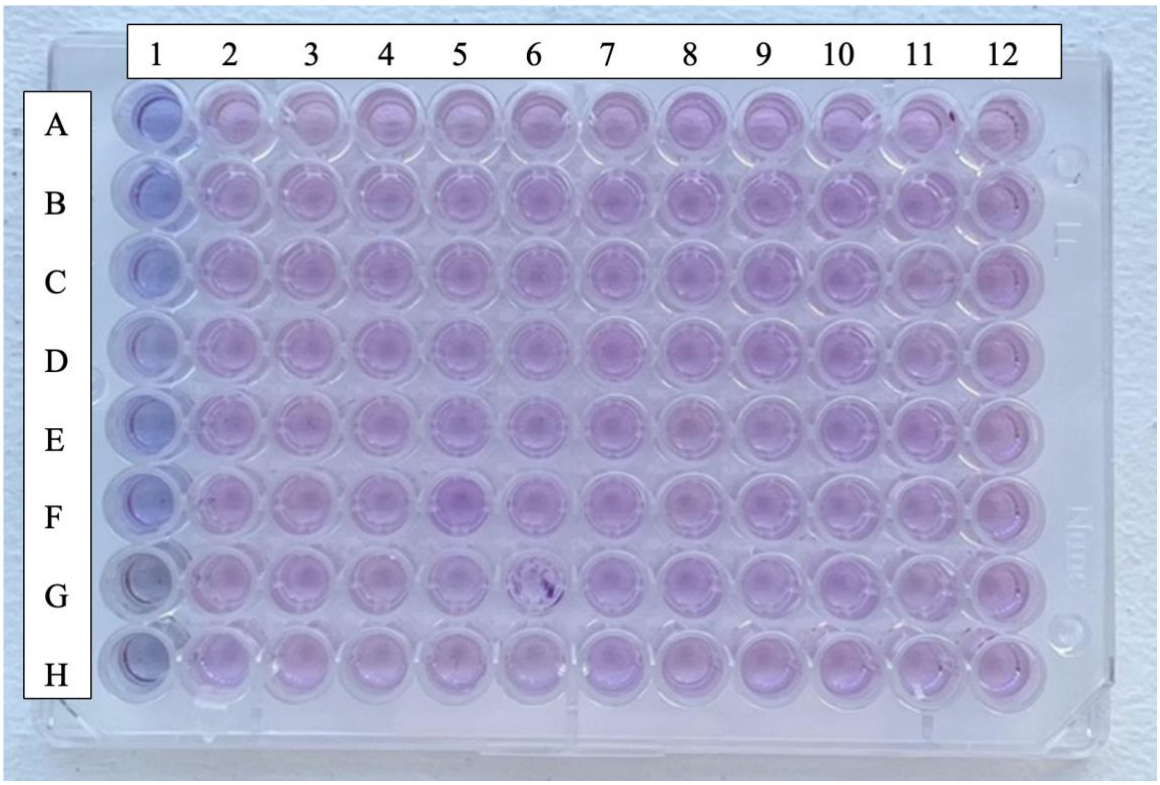

Figure 9: Positive control is in Column 1, treatment was identical to samples, but supernatant was extracted from *P. putida* F1 grown with toluene exposed to DFBD at 80µM in Rows G & H, 70µM in Rows F & E, 60µM in Rows D & C, and 40µM in Rows B & A. Column 12 was negative control, the same treatment as samples but with HEPES (Rows E-F) or H2O (Rows A-D) instead of supernatant. Bacterial dilutions originated from the Korsør test center (Columns 2,3,7 and 8), Gangro Beach (Columns 4,5,9 and 10), and Korsør Nor (Columns 6 & 11). Samples ranged from undiluted (Row H) to 10-7 (Row A). All bacteria were grown in LB media.

3.3.2 Trial Two

The second colorimetric screening assay assessed different media and carbon sources for bacterial growth to see if cultivation conditions differentially selected for degradation of PFOA and the detection of fluoride via colorimetric assay. The colorimetric assay is shown in Figure 10. Various pink wells were observed in Plate 2, which used M9 media for bacterial growth. This pink color was suggestive of an interference in the assay. Residual M9 media may have remained as cells were resuspended in HEPES buffer, and one or more of these components may have reacted with the chemicals in the colorimetric assay to create an unusual pink tone. In the initial paper describing the colorimetric screening assay, various buffers, and growth media components were evaluated for interference, and one that was found to strongly interfere was 10 mM sodium phosphate monobasic (Bygd et al., 2022). M9 media contains both monobasic and dibasic sodium phosphate, which is likely the cause of the interference.

Based on the colorimetric assay results from plate one, a darker shade of purple in wells E8 and F8 was observed visually, as can be seen in Figure 10. Subsequent spectrophotometer readings showed the highest absorbance for 620 nm in wells 10A and 10B, as shown in Table 8. Both wells had dilutions from the same bacterial sample, originally sourced from Site 1 Clay Subsoil. This could reflect the presence of a microbe with particularly adept PFOA degradation abilities in this environmental sample compared to the others. Other notable wells based on their high absorbance at 620 nm included wells 8A, 5A, and 5B.

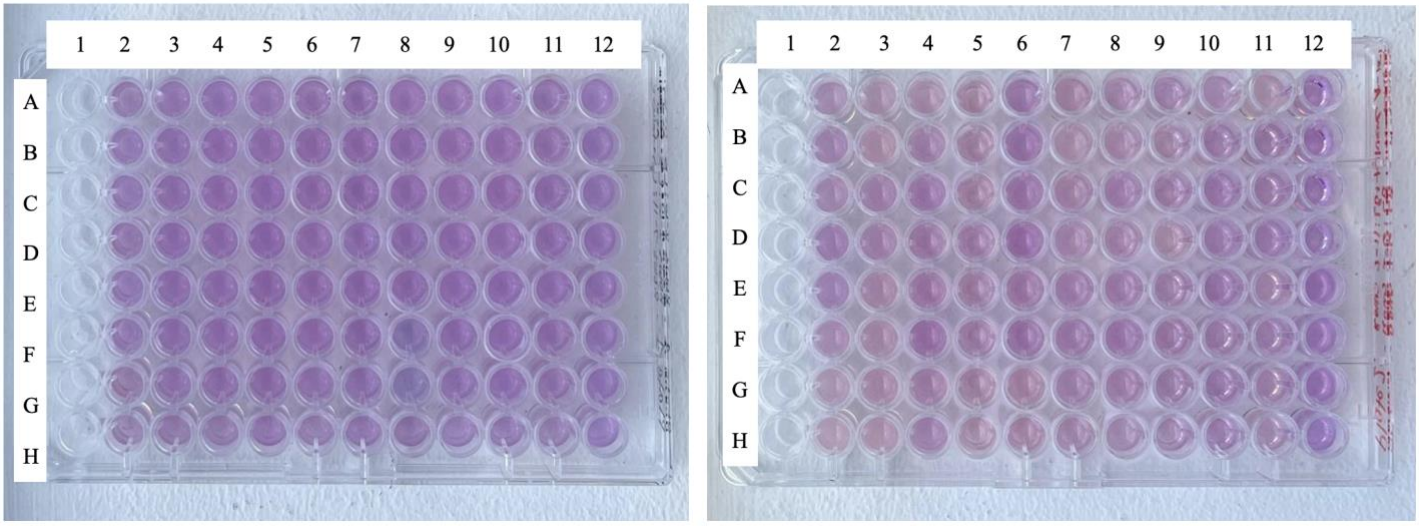

Figure 10: Plate 1 (left) had bacterial samples grown in LB media: columns 2-6 with just LB, and columns 7-11 with LB and 1µL toluene. Plate 2 (right) contains bacterial samples grown in M9 media: columns 2-6 with MCPA as the carbon source, and columns 7-11 with glucose. Both plates have undiluted samples in row H, with tenfold serial dilutions to 10-7 in row A. Bacterial sources for both plates are: columns 2,3,7 and 8 from Korsør test center, columns 4 & 9 from Site 1 Clay Subsoil, columns 5 & 10 from Site 1 Middle Zone Soil, and rows 6 & 11 from Site 1 Top Soil. Row 12 contains negative controls. Positive controls were not included.

Spectrophotometer readings of plate one revealed a trend of generally higher 620 nm absorbance moving toward the top of the plate. As shown by the numbers and color gradient in Table 8, readings tended to be higher closer to row A and lower closer to row H for each respective column. This trend mirrors the dilution pattern utilized during sample preparation, suggesting that bacterial dilutions at a sevenfold magnitude may have been more conducive to degradation, as signaled by the larger spectrophotometer reading, which is associated with a darker purple and therefore, a higher likelihood of free fluoride resulting from PFOA degradation. This trend was especially prevalent in columns ten and five. This phenomenon could be explained by reduced competition for resources from bacteria that are not capable of PFOA degradation in the samples with more dilution. While the sourcing of environmental bacteria from PFAS sites, as well as the incubation of these bacterial communities with PFOA, with or without the addition of toluene, served to select for bacteria capable of degrading or tolerating, PFOA, resource competition in samples with higher initial bacterial abundance could see reduced signs of degradation due to the diversion of resources to non-degrading bacterial species also present in the sample.

	2	3	4	5	6	7	8	9	10	11	12
A	0.313	0.472	0.526	0.643	0.312	0.202	0.655	0.337	0.782	0.283	0.377
B	0.343	0.482	0.465	0.623	0.476	0.291	0.46	0.452	0.745	0.404	0.337
C	0.408	0.471	0.473	0.562	0.396	0.255	0.528	0.55	0.557	0.495	0.508
D	0.324	0.445	0.41	0.608	0.437	0.209	0.366	0.48	0.467	0.351	0.38
E	0.37	0.517	0.465	0.6	0.335	0.295	0.299	0.572	0.438	0.5	0.342
F	0.286	0.47	0.439	0.531	0.447	0.186	0.352	0.33	0.497	0.383	0.429
G	0.412	0.464	0.416	0.485	0.497	0.238	0.421	0.4	0.344	0.396	0.37
H	0.461	0.52	0.508	0.66	0.455	0.286	0.305	0.424	0.374	0.436	0.366

Table 8: Absorbance readings at 620 nm for plate one.

Evaluation of the 530nm/620nm absorbance ratios, presented in Table 9, revealed that many wells had an absorbance ratio of .7 or higher, the ratio used in the previous study to qualify a well as likely to have fluoride (Bygd et al., 2022). In this trial, 20 out of the 80 sample wells exceeded this ratio, suggesting a potential for bacteria capable of defluorination in these samples. Half of the wells with an absorbance ratio over .7 were found in either column three or column five. This observation could indicate that certain bacterial communities from the environmental samples may have been more effective degraders than others.

The highest ratio observed was .8 in well 3E. However, negative controls in column twelve also showed relatively high ratios, around .6. Several sample wells, including all of column seven, had lower ratios than the controls, which could suggest that the .7 absorbance ratio is not an effective indicator of color change in this experiment and instead falls within the normal range for the unbound complex. The lack of a positive control in this study further complicates interpretation. However, Figure 8 in section 3.2.3 shows the earliest fluoride concentrations did have an absorbance ratio of around .7, while the negative control also showed an absorbance ratio of .6, consistent with the results in Table 9. Higher amounts of fluoride tend to have an absorbance ratio over one, which was not seen in this experiment, so a fluoride concentration over 1 ppm and significant defluorination is unlikely in this assay. However, it is still possible that the interesting patterns observed in the absorbance ratios and the 620 nm absorbance readings are evidence for small amounts of free fluoride released in the system. Future experiments could be conducted to better determine the accuracy with which the colorimetric assay can detect free fluoride in small quantities resulting from defluorination by biological systems.

	2	3	4	5	6	7	8	9	10	11	12
A	0.61	0.71	0.71	0.71	0.58	0.58	0.72	0.60	0.69	0.62	0.61
B	0.65	0.72	0.66	0.73	0.67	0.65	0.69	0.66	0.75	0.63	0.62
C	0.74	0.71	0.65	0.68	0.64	0.55	0.69	0.70	0.67	0.57	0.65
D	0.63	0.69	0.66	0.71	0.67	0.54	0.64	0.67	0.64	0.56	0.62
E	0.65	0.79	0.67	0.62	0.58	0.61	0.62	0.69	0.65	0.63	0.59
F	0.60	0.65	0.65	0.68	0.62	0.47	0.64	0.63	0.68	0.58	0.63
G	0.66	0.73	0.65	0.67	0.57	0.48	0.70	0.60	0.60	0.53	0.62
H	0.70	0.70	0.73	0.74	0.66	0.57	0.62	0.62	0.59	0.64	0.62

Table 9: Absorbance ratios for 530 nm / 620 nm for plate one.

Based on the observations noted in this experiment, samples were selected for further investigation via genome sequencing and chemical analysis. The samples selected were from wells: 3E, 5A, 5B, 5C, 5D, 5E, 5F, 5G, 5H, 8A, 8G, 8H, 10A, 10B.

3.4 Sequencing

DNA extraction and nanopore sequencing were only successful for samples from a few of the identified wells. The resulting sequences were analyzed using CLC Genomics Workbench to identify 16S RNA sequences, which were referenced using BLAST against the NCBI GenBank non-redundant database to identify bacteria likely present in the samples. The results from this analysis are shown below in Table 10. Sequence similarity between genes related to defluorination enzymes from literature and those found in our samples is described in Table 11.

CA Well	Scientific Name	Percent Identity	Query Cover	Accession Number
5H	Pseudomonas sp. S07E 245	99.55%	100%	CP080625.1
	Pseudomonas sp. 02C 26	99.58%	100%	CP025262.1
5E	Stenotrophomonas maltophilia	100.00%	100%	CP052863.1
	Pseudomonas fluorescens	99.61%	100%	OZ024668.1
5D	Stenotrophomonas indicatrix	99.37%	100%	CP124546.1
	Pseudomonas fluorescens	100.00%	100%	OZ024668.1
	Stenotrophomonas sp. MYb57	99.14%	100%	CP023271.1
	Buttiauxella sp. R73	99.15%	100%	CP133838.1
5C	Paraburkholderia fungorum	100.00%	100%	CP099647.1
	Delftia acidovorans	100.00%	100%	CP022656.1
	Aeromonas media WS	98.40%	100%	CP007567.1
10B	Stenotrophomonas maltophilia	100.00%	100%	CP044092.1
	Pseudomonas sp. ADAK20	98.83%	100%	CP052858.1
	Pseudomonas sp. B14-6	100.00%	100%	CP053929.1
8F	Stenotrophomonas maltophilia	100.00%	100%	CP040440.1
	Serratia sp. 3ACOL1	98.71%	100%	CP033055.1
	Pseudomonas sp. S35	99.03%	100%	CP019431.1
8G	Pseudomonas protegens	99.09%	100%	CP031396.1
	Stenotrophomonas maltophilia	100.00%	100%	CP040440.1
	Pseudomonas sp. ML2-2023-3	100.00%	100%	CP146343.1

Table 10: Best match results of 16S RNA sequences found from nanopore sequencing of select samples. CA refers to the well of the colorimetric assay.

CA Cell	Hit	Description	E-value	HSP length	% Identity
5H	WP_020793433.1	LLM class flavin-dependent oxidoreductase [*Gordonia* sp. NB41Y]	5.01E-66	220	55.36
5E	WP_238404007.1	MULTISPECIES: alcohol dehydrogenase catalytic domain-containing protein [*Gordonia*]	4.50E-38	326	35.42
	WP_020793433.1	LLM class flavin-dependent oxidoreductase [*Gordonia* sp. NB41Y]	1.17E-37	207	40
5D	WP_020793433.1	LLM class flavin-dependent oxidoreductase [*Gordonia* sp. NB41Y]	1.29E-83	318	48.92
	WP_053776268.1	NAD(P)-dependent alcohol dehydrogenase [*Gordonia* sp. NB41Y]	2.40E-81	256	48.45
5C	ABG94339.1	alkane 1-monooxygenase [*Rhodococcus jostii* RHA1]	1.39E-79	179	61.67
	WP_020793433.1	LLM class flavin-dependent oxidoreductase [*Gordonia* sp. NB41Y]	4.89E-63	317	45.45
10B	WP_053776268.1	NAD(P)-dependent alcohol dehydrogenase [*Gordonia* sp. NB41Y]	1.06E-96	342	50.58
8F	WP_053776268.1	NAD(P)-dependent alcohol dehydrogenase [*Gordonia* sp. NB41Y]	2.92E-81	295	50.51
8G	WP_053776268.1	NAD(P)-dependent alcohol dehydrogenase [*Gordonia* sp. NB41Y]	2.24E-96	342	50.58
	WP_269074981.1	LLM class flavin-dependent oxidoreductase [*Dietzia aurantiaca*]	2.14E-95	374	47.61
	WP_020793433.1	LLM class flavin-dependent oxidoreductase [*Gordonia* sp. NB41Y]	5.05E-82	299	49.34

Table 11: Best match results for a BLAST search of enzymes of interest based on previous defluorination studies and the sequencing results of genes from environmental samples associated with potential PFOA degradation in the colorimetric assay

Sequencing data from the environmental samples revealed the presence of several notable bacterial species that have been identified in previous studies as significant for pollutant bioremediation in general and even PFAS biodegradation specifically. These include, strains of *Pseudomonas* and *Strenotrophomonas*, as well as, *Delftia acidovorans,* and *Paraburkholderia fungorum*.

3.4.1 *Pseudomonas*

The *Pseudomonas* genus is known for its diverse metabolic abilities and widespread environmental range, making it well-studied in the field of bioremediation (F. Hu et al., 2023). *Pseudomonas* presence in our samples was robust, with 9 bacterial species out of the 20 identified belonging to this genus.

The species identified in wells 5E and 5D of the colorimetric assay, *Pseudomonas fluorescens*, is particularly relevant in this study as it has been previously demonstrated to break the carbon-fluorine bond in the naturally occurring fluorinated compound, sodium fluoroacetate (Camboim et al., 2012; Leong et al., 2017). A different study also identified the release of fluoride ions after *Pseudomonas fluorescens* incubation with PFOA for a duration of 58 hours (Harris et al., 2022). The strain, in addition to two other *Pseudomonas* strains, has been shown to transform fluorotelomer alcohols (FTOH) and polyfluoroalkyl phosphates (6:2 PAP) (Lewis et al., 2016). The study even suggested that these bacteria are able to utilize the substances as substrates rather than degradation occurring due to cometabolism (Lewis et al., 2016). The *Pseudomonas fluorescens* strain has also been recognized for its hydrocarbon bioremediation potential due to its ability to generate biosurfactants (Gutiérrez et al., 2020). The combination of hydrocarbon bioremediation ability and ability to break carbon fluorine bonds under certain circumstances make *Pseudomonas fluorescens* an interesting candidate for the degradation of PFOA in wells 5E and 5D, which each saw around 66% PFOA reduction, as shown in Table 12, in section 3.5.1. This bacteria's presence in both wells, which had bacterial dilutions from the same soil sample sourced from Gangro Beach in Korsør, is additional evidence of its ability to survive in highly PFAS-contaminated environments.

Other species from the *Pseudomonas* genus have also been accredited with remarkable defluorination activity. One study found that *Pseudomonas aeruginosa* isolated from wastewater treatment sludge decomposed 67% of PFOS after 48 hours of incubation (Kwon et al., 2014). Another species, *Pseudomonas parafulva,* isolated from a contaminated site, was found to degrade 48.1% of PFOA (Yi et al., 2016). *Pseudomonas plecoglossicida* isolated from polluted soil was able to use PFOS as a sole carbon and energy source, with evidence of broken C-F bonds as shown by the presence of free fluorine (Chetverikov et al., 2017). Inoculation of this bacteria in contaminated soil was even shown to reduce PFOS quantity by 75% over the course of 3 months (Chetverikov et al., 2017). Given the relative abundance of *Pseudomonas* identified in our samples and their relation to known PFAS degrader species, it is possible these bacteria have an exceptional capability to either tolerate or metabolize the PFOA used in our study.

3.4.2 *Delftia acidovorans and Paraburkholderia fungorum*

Delftia acidovorans is another notable bacterium identified in our samples due to its previously demonstrated PFAS degradation activity. This species was isolated from PFAS-contaminated soils in Colorado, USA, where it was able to grow in minimal media with PFOA as the sole carbon source, resulting in the release of around 2.4mg/L of fluoride as detected by a fluoride ion probe (Harris et al., 2022). The study attributed PFOA degradation by *Delftia acidovorans* to genes coding for two haloacid dehalogenases (Harris et al., 2022). The same dehalogenase genes have been shown in *Delftia acidovorans* to code for enzymes that can degrade the naturally occurring fluorinated compound fluoroacetate (Leong et al., 2017). The responsible dehalogenases are encoded by two different genes on its 65 kb plasmid pUO1 (Leong et al., 2017). A search of the genome found in this well of the colorimetric assay, 5C, was conducted using Blastx to look for homologous genes. A 99% identity match with haloacid dehalogenase type II, WP_030099003.1 was identified. The presence of this gene could indicate defluorination abilities that expand beyond the fluoroacetate substrate. Modeling of haloacid dehalogenases showed a highly conserved region with a high PFOA binding score of -6.7 (Harris et al., 2022). The haloacid dehalogenase coding genes identified in well 5C of our sample were attributed to the other bacterial species found in that well, *Paraburkholderia fungorum*.

The *Paraburkholderia fungorum* identified in well 5C of the colorimetric assay is related to the *Burkholderia* sp. FA1, from which the first three-dimensional structure of fluoroacetate dehalogenase was determined (Seong et al., 2019). The fluoroacetate dehalogenase in *Burkholderia* sp. FA1 has high substrate specificity for fluoroacetate compared to chloroacetate (Leong et al., 2017). It was found that the fluorine was stabilized by hydrogen bonds to His149, Trp150, and Tyr212 of *Burkholderia* sp. FA1 strain, lowering the activation energy to cleave the C-F bond to only 2.7 kcal/mol (Leong et al., 2017).

Additionally, both the *Delftia acidovorans and Paraburkholderia fungorum* strains have been associated with the biodegradation of another group of recalcitrant environmental pollutants, polycyclic aromatic hydrocarbons (PAHs) (J. Li et al., 2024). The colorimetric assay well with these bacteria, 5C, was also analyzed in CLC Genomics Workbench to compare the genomes against known genes associated with defluorination enzymes. The closest match was found in this sample, with a 62% identity match for alkane 1-monooxygenase, as shown in Table 11. This enzyme is of interest as it was overexpressed in an experiment where *Pseudomonas sp.* strain

273 grew and released fluoride with the fluoroalkane, 1,10-difluorodecane (DFD) as the sole carbon and energy source in oxic conditions (J. Xiao et al., 2023). The presence of these two bacteria known to have capabilities to break C-F bonds, along with the similarity between genes encoding for defluorination enzymes and those in well 5C, is a signal of the selective pressure of our experimental design and supports the possibility for defluorination activity as the explanation for the outcome of the colorimetric assay.

3.4.3 *Stenotrophomonas*

Bacteria from the *Stenotrophomonas* genus were also commonly identified in our samples, with a presence in five out of seven samples with genetic information available. This genus is known for its ability to biodegrade environmental pollutants. *Stenotrophomonas indicatrix*, as found in well 5D, has been identified as a significant degrader of phenanthrene (PHE), which is a PAH composed of three benzene rings (J. Li et al., 2024). This strain was isolated from industrial soil and was found to degrade nearly all PHE after 30 days of incubation (Lara-Moreno et al., 2023). The study accredits oxygenase activity with the first step of hydrocarbon metabolism, which is also important for PFAS degradation. Twenty-two oxygenases were identified on the genome of *Stenotrophomonas indicatrix* (Lara-Moreno et al., 2023). Analysis of the bacterial genomes from the samples showed similarity between the genes in sample 5D, which had the 16S RNA match to *Stenotrophomonas indicatrix*, and genes encoding an LLM class flavin-dependent oxidoreductase. This enzyme has been previously identified as relevant to PFAS metabolism due to its upregulation in a transcriptomic study that looked at gene expression in *Gordonia sp*. strain NB4-1Y exposed to two PFAS compounds, 6:2 fluorotelomer sulfonate and (6:2 FTSA) and 6:2 fluorotelomer sulfonamidoalkyl betaine (6:2 FTAB) (Bottos et al., 2020).

The *Stenotrophomonas maltophilia* was the most commonly found species in the samples, with a presence in 4 out of 7 samples. This species was found in wells with bacterial incubations sourced from geographically separate places, both the Site 1 Middle Zone soil and soil from the Korsør test center, which could imply a particular aptitude to surviving in PFAS-contaminated soils. The species has also been previously studied for bioremediation.

Stenotrophomonas maltophilia strain W18 was found to be able to degrade 60% of fluoranthene, a type of PAH, in 10 days (Y. Xiao et al., 2021). Genes coding for alcohol dehydrogenases were identified as important by relative expression for fluoranthene degradation (Y. Xiao et al., 2021).

Sample 5E, which had identified *Stenotrophomonas maltophilia* in it, also showed a 35% identity match based on a Blast search for relatedness conducted in CLC Genomics Workbench between a gene sequence coding for an alcohol dehydrogenase that had been linked to PFAS degradation in a transcriptomic study and those found the sample (Bottos et al., 2020). While the percent identity match is somewhat low, 35%, there is the possibility of the genetics coding for a similar enzyme, which could also support degradation, as this species has been identified as a strong degrader organism, even for halogens. A bacterial consortium isolated from contaminated soil with the strain *S. maltophilia* was shown to degrade highly chlorinated aromatic compounds such as PCBs, significantly reducing the ecotoxicity of contaminated soils (Horváthová et al., 2018). The consistent detection of the *Stenotrophomonas* genus in our samples, coupled with its well-recognized ability for biodegradation of recalcitrant pollutants, provide supporting evidence of potential microbial PFAS degradation in this study.

It is relevant to note that while these bacteria are intriguing for their potential in PFAS degradation, some have also been identified as antibiotic-resistant and opportunistic human pathogens, which could have implications for their ability to be used in bioremediation efforts down the line. However, at this stage of the research, it is relevant to consider all bacteria exhibiting potential defluorination capacity.

3.5 Chemical Analysis

3.5.1 Chemical Analysis Results

Sample	% PFOA lost
3B	54.3
3C	48.6
3E	42.9
6B	71.4
10A	54.3
10B	51.4
8A	65.7
8F	68.6
8G	65.7
5A	65.7
5B	65.7
5C	65.7
5D	65.7
5E	65.7
5F	65.7
5G	65.7
5H	62.9

Table 12: Percentage of PFOA lost represents the difference between samples and control in PFOA as detected by LC-HRMS/MS. Samples are referred to by the associated well in Trial 2 of the colorimetric screening assay. Samples in bold have genetic sequencing data.

3.5.2 Chemical Analysis Discussion

Chemical analysis of the samples revealed significant differences in the amount of PFOA detected in samples when compared to the control. All samples showed PFOA reduction in comparison to control, ranging between 43% and 71%, as shown in Table 12. The control sample used for comparison was prepared with the same amount of HEPES and PFOA as the samples but was never exposed to bacteria. Therefore, comparison between the samples and this control can give insight into the effect of bacterial intervention on PFOA fate in this experiment.

Along with the reduction of PFOA in the samples compared to the control, a parallel effect was observed with perfluorohexanoic acid (PFHxA) and perfluoroheptanoic acid (PFHpA), which are other PFAS compounds also detected in this experiment. PFHxA and PFHpA were not added intentionally in this study and their documented presence could be the result of PFOA degradation as they are likely candidates to be PFOA metabolites. Alternatively, they could be the result of impurities from the PFOA used in this experiment, which was purchased at 96% purity.

PFOA, PFHxA, and PFHpA quantities were found to be smaller in all samples than in the positive control, with a strong correlation observed between all three of these compounds. Graphs illustrating this phenomenon are included in Figures 13, 14, and 15 of the supplementary materials. In contrast, another PFAS compound, sodium perfluorohexanesulfonic acid (L-PFHxS), was found to have close to a 1:1 ratio between all samples and the control. PFOA, PFHxA, and PFHpA are all PFCAs due to their carboxylic groups. They have eight, seven, and six carbon chains, respectively. L-PFHxS is a six carbon-chain PFSA due to its sulfonic acid group. The difference in their fate in this experiment could be a result of their varying chemical properties.

The lower amount of PFOA, PFHxA, and PFHpA identified in samples when compared to controls may have been due to the sorption of these compounds on the bacterial cells during the experimental process. This would result in their altered distribution throughout the sample after the centrifuge step, as they would be overrepresented in the bacterial pellet rather than in the 100µL of supernatant that was extracted for chemical analysis. This could explain the high percentages of reduction we see when comparing PFOA in samples to controls, but it also does not rule out the possibility of concurrent degradation. Notably, there is variation in PFOA/PFHxA and PFOA/PFHpA ratios grouped by environmental sample. Box plots of these data, available for reference as Figures 16 and 17 in the supplementary materials, show that these ratios have different ranges for each sample group. This could imply that the different groups experience reduction of these compounds differently, which could be related to microbe-mediated degradation, rather than simple sorption. However, the lack of data available for all the different dilution ranges for each environmental sample is a limitation, as the average amount of bacteria could have been different and caused the different effects. Future studies could evaluate OD600 of the samples grown with PFOA, and better track growth dynamics.

Further evidence to support degradation comes from the presence of perfluoro-n-butanoic acid (PFBA) in two of the samples from wells 5G and 6B. Notably, this compound was not found in the control. PFBA is a PFCA with a carbon-chain length of four, which could be the result of PFOA degradation. PFOA degradation tends to begin with the non-fluorinated carboxyl group at the α position, which is generally the weakest point in this chemical structure (Shahsavari et al., 2021). From this point, a series of biologically mediated and spontaneous reactions can ensue, eventually resulting in the reduction of PFOA by one CF_2 unit, which is a process that can be repeated, eventually generating shorter chain PFCAs, such as PFBA, as the terminal products (J. Xiao et al., 2023). Additionally, hydrogen-substituted perfluoroalkanes or perfluoroalkyl alcohols, perfluoroalkyl aldehydes, hydrogen-containing fluorinated carboxylic acids, and unsaturated fluorinated hydrocarbons are other likely metabolites (J. Xiao et al., 2023). Further details on potential pathways of PFOA degradation through combined biological and physiochemical metabolism are provided in Figure 11 of the supplementary materials.

The volatility of PFAS tends to increase as chain length decreases, a phenomenon that may explain the absence of an increase in measured degradation products in our samples compared to the control. A degree of degradation may have occurred in the samples, as evidenced by the colorimetric assay, varying PFOA/PFHxA, and PFOA/PFHpa ratios by sample group, and the presence of PFBA in two of the samples. However, the current data is limited. In order to gain a more robust understanding of the PFOA fate, future studies could add isotope-labeled PFOA from the initial incubation stage and use scintillation counting techniques to better delineate the fate of PFOA within this experimental set-up. In another study, fluoride balance has been achieved to successfully account for degradation activity by tracking total fluorine in the original compound (PFOA or PFOS), their shorter carbon chain PFAAs intermediates, and fluoride ions in solution (Jaffé et al., 2024). Quantifying the formation of transformation products and reduction of substrate could allow for mass balance calculations, which would also give a better understanding of degradation pathways and the effect of sorption.

While further studies are needed to truly elucidate PFOA fate, based on the evidence of this study, the possibility proposed in this thesis, is that most PFOA was sorbed to bacterial cells, while a smaller portion was degraded by bacteria from the environmental samples. The amount of PFOA utilized in this study was quite high, which may have limited degradation due to the toxicity of fluoride produced. In this experiment, bacteria were incubated with around 3.64 mM PFOA, which has 15 fluorine atoms per molecule. Meanwhile, as little as 0.1mM fluoride has

been shown to have inhibitory effects on essential enzymes (Wackett, 2024). Reducing PFOA concentration in future experiments could allow for a greater percentage of degradation to occur before toxicity and for better tracking of PFOA fate. The degradation of PFAS may be inherently toxic to the bacteria capable of doing it, but overexpression of the genes related to these mechanisms may still cause it to occur. This is an important area for additional research. Furthermore, understanding bacterial fitness to fluoride stress is also a key research area related to the biodegradation of PFAS.

3.6 Merged Project Discussion

With the goal of better understanding relationships amongst the varying data produced through the course of this project, analysis comparing certain factors was conducted. To see if there was a connection between the amount PFOA was reduced during the experiment as determined by chemical analysis, and the degree of color change in the assay, spectrophotometer readings were compared to PFOA percentage lost per sample. These metrics were not found to be significantly correlated. This could be explained by incomplete degradation of PFOA via various routes, which may cause the release of fluoride ions in a manner that is not always proportional to the amount of PFOA that is lost. Bacteria may synthesize different enzymes that catalyze different degradation routes, some of which may be more likely to release free fluoride, while others might tend to produce other intermediate degradation products that do not bind to the alizarin-lanthanum complex. Additionally, if such intermediates are volatile, it could have prevented their detection via chemical analysis in this study. The specific degradation pathway may have differed by sample, resulting in either more or less fluoride, changing the spectrophotometer readings accordingly but not necessarily reflecting the total amount of PFOA lost.

Notably, eight of the wells with chemical analysis data exhibited high similarity, with a 65.7% PFOA reduction in samples compared to the control, as shown in Table 12 of section 3.5.1. Of these wells, seven were from the same bacterial sample, sourced from Site 1 Middle Zone soil. Despite their consistency in the percentage of PFOA lost and their original source, genetic sequencing identified different bacteria in each well. The one exception was *Pseudomonas fluorescens*, which was found in both 5E and 5D, as shown in Table 10 of section 3.4. Horizontal gene transfer could be one explanation for the observed similarity. Degradative abilities could have been transferred among the different bacterial species prior to their separation into different

dilutions, which could also explain why some entire columns in Tables 8 and 9 in section 3.3.2 tend to have higher absorbance readings and ratios than other entire columns.

Mobile genetic elements are versatile bacterial tools that can accelerate evolutionary adaptiveness to the stress of a new compound in the environment. The environmental half-life of the herbicide atrazine was significantly reduced through a related mechanism. A series of point mutations gave rise to a novel dechlorinase enzyme from a deaminase gene, and as additional genes assembled, a metabolic pathway to degrade the compound was formed, being found on plasmids with nearly identical sequences over six continents (Wacket, 2024). Similarly, antibiotic resistance genes may require overexpression related to mobile genetic elements to confer resistance (Nielsen et al., 2022).

The transfer of genetic material among the bacterial community found in this environmental sample is one possible explanation for the similar degradation percentages observed in these samples. Genes coding for a LLM class flavo-dependent oxoreductase had an identity match ranging from 40% to 55% in all of these samples. While these percent identity matches are low between the genes in the samples and the genes coding for this oxoreductase, the connection between these genes and all samples shows that there may be similarity amongst the genes in these samples, which could exceed their relationship to the genes encoding the enzyme itself. Further analysis of the relationship between the degradation-related genes between samples and the genetic context of these genes can shed light on the degree of mobilization that may have occurred.

Overall, this project utilized a variety of microbial and chemical techniques, resulting in a diverse data set. Additional analysis could focus on coordinating the data produced throughout the workflow of this experiment to better visualize connections between bacteria, genetic sequences, spectrophotometer readings, and the results of chemical analysis. After the collection of additional data, coordination amongst the parameters could provide insight into the relationships at play amongst the different experimental components, which could guide further optimization of the process and understanding of microbial degradation of PFAS.

Conclusion

This thesis has contributed to advancing the understanding of PFAS biodegradation, a significant area of research given the widespread, toxic, and persistent nature of these pollutants. Such preliminary research is fundamental to the potential development of a cost-effective and environmentally friendly bioremediation approach for these compounds in the future. The work in this thesis corroborated the results of a known defluorination reaction and screened bacterial dilutions from environmental samples for signs of PFAS degradation using a colorimetric assay. Colorimetric assay results showed relevant patterns and were indicative of potential PFAS degradation. Chemical analysis of samples showed reduced amounts of PFOA in all samples compared to a control with no bacterial exposure. Together, these experiments showed supporting evidence for the potential that a small amount of PFOA degradation had occurred. Genetic sequencing revealed a variety of intriguing species and genera that had been linked to the biodegradation of PFAS and other pollutants in previous studies, including *Pseudomonas fluorescens, Delftia acidovorans, Paraburkholderia fungorum*, and *Stenotrophomonas maltophilia*. Although the data collected was limited, preventing definitive conclusions about PFOA degradation, the study offers encouraging evidence for this possibility and provides a basis for continued exploration into the capacity of microbes for PFAS biodegradation via colorimetric assay.

References

Beck, I. H., Bilenberg, N., Andersen, H. R., Trecca, F., Bleses, D., & Jensen, T. K. (2023). Association between prenatal or early postnatal exposure to perfluoroalkyl substances and language development in 18 to 36-month-old children from the Odense Child Cohort. *Environmental Health: A Global Access Science Source*, *22*(1). https://doi.org/10.1186/s12940-023-00993-w

Booten, C., Nicholson, S., Mann, M., & Abdelaziz, O. (2014). *Refrigerants: Market Trends and Supply Chain Assessment*. www.osti.gov/scitech

Bottos, E. M., AL-shabib, E. Y., Shaw, D. M. J., McAmmond, B. M., Sharma, A., Suchan, D. M., Cameron, A. D. S., & Van Hamme, J. D. (2020). Transcriptomic response of Gordonia sp. strain NB4-1Y when provided with 6:2 fluorotelomer sulfonamidoalkyl betaine or 6:2 fluorotelomer sulfonate as sole sulfur source. *Biodegradation*, *31*(4–6), 407–422. https://doi.org/10.1007/s10532-020-09917-8

Boyd, R. I., Ahmad, S., Singh, R., Fazal, Z., Prins, G. S., Madak Erdogan, Z., Irudayaraj, J., & Spinella, M. J. (2022). *Toward a Mechanistic Understanding of Poly-and Perfluoroalkylated Substances and Cancer*. https://doi.org/10.3390/cancers

Buck, R. C., Franklin, J., Berger, U., Conder, J. M., Cousins, I. T., Voogt, P. De, Jensen, A. A., Kannan, K., Mabury, S. A., & van Leeuwen, S. P. J. (2011). Perfluoroalkyl and polyfluoroalkyl substances in the environment: Terminology, classification, and origins. *Integrated Environmental Assessment and Management*, *7*(4), 513–541. https://doi.org/10.1002/ieam.258

Bygd, M. D., Aukema, K. G., Richman, J. E., & Wackett, L. P. (2021a). Unexpected Mechanism of Biodegradation and Defluorination of 2,2-Difluoro-1,3-Benzodioxole by Pseudomonas putida F1. *MBio*, *12*(6). https://doi.org/10.1128/mBio.03001-21

Bygd, M. D., Aukema, K. G., Richman, J. E., & Wackett, L. P. (2021b). Unexpected Mechanism of Biodegradation and Defluorination of 2,2-Difluoro-1,3-Benzodioxole by Pseudomonas putida F1. *MBio*, *12*(6). https://doi.org/10.1128/mBio.03001-21

Bygd, M. D., Aukema, K. G., Richman, J. E., & Wackett, L. P. (2022). Microwell Fluoride Screen for Chemical, Enzymatic, and Cellular Reactions Reveals Latent Microbial

Defluorination Capacity for 2CF3 Groups. *Applied and Environmental Microbiology*, *88*(9). https://doi.org/10.1128/aem.00288-22

Camboim, E. K. A., Almeida, A. P., Tadra-Sfeir, M. Z., Junior, F. G., Andrade, P. P., McSweeney, C. S., Melo, M. A., & Riet-Correa, F. (2012). Isolation and identification of sodium fluoroacetate degrading bacteria from caprine rumen in Brazil. *The Scientific World Journal*, *2012*. https://doi.org/10.1100/2012/178254

Carsten Lassen, Allan Astrup Jensen, Alexander Potrykus, Frans Christensen, Jesper Kjølholt, Christian Nyander Jeppesen, Sonja Hagen Mikkelsen, & Sally Innanen. (2013). *Survey of PFOS, PFOA and other perfluoroalkyl and polyfluoroalkyl substances*. Miljøstyrelsen.

Chetverikov, S. P., Sharipov, D. A., Korshunova, T. Y., & Loginov, O. N. (2017). Degradation of perfluorooctanyl sulfonate by strain Pseudomonas plecoglossicida 2.4-D. *Applied Biochemistry and Microbiology*, *53*(5), 533–538. https://doi.org/10.1134/S0003683817050027

Danish Veterinary and Food Administration. (n.d.).

De Silva, A. O., Armitage, J. M., Bruton, T. A., Dassuncao, C., Heiger-Bernays, W., Hu, X. C., Kärrman, A., Kelly, B., Ng, C., Robuck, A., Sun, M., Webster, T. F., & Sunderland, E. M. (2021). PFAS Exposure Pathways for Humans and Wildlife: A Synthesis of Current Knowledge and Key Gaps in Understanding. In *Environmental Toxicology and Chemistry* (Vol. 40, Issue 3, pp. 631–657). Wiley Blackwell. https://doi.org/10.1002/etc.4935

Donnelly, C., & Murphy, C. D. (2009). Purification and properties of fluoroacetate dehalogenase from Pseudomonas fluorescens DSM 8341. *Biotechnology Letters*, *31*(2), 245–250. https://doi.org/10.1007/s10529-008-9849-4

ECHA. (n.d.). *Annex XV Restriction Report: Per-and polyfluoroalkyl substances (PFASs)*.

EEA. (2019). *Emerging chemical risks in Europe- PFAS*.

Evich, M. G., Davis, M. J. B., McCord, J. P., Acrey, B., Awkerman, J. A., Knappe, D. R. U., Lindstrom, A. B., Speth, T. F., Tebes-Stevens, C., Strynar, M. J., Wang, Z., Weber, E. J., Henderson, W. M., & Washington, J. W. (2022). Per- and polyfluoroalkyl substances in the environment. *Science*, *375*(6580). https://doi.org/10.1126/science.abg9065

Fenton, S. E., Ducatman, A., Boobis, A., DeWitt, J. C., Lau, C., Ng, C., Smith, J. S., & Roberts, S. M. (2021). Per- and Polyfluoroalkyl Substance Toxicity and Human Health Review: Current State of Knowledge and Strategies for Informing Future Research. In *Environmental Toxicology and Chemistry* (Vol. 40, Issue 3, pp. 606–630). Wiley Blackwell. https://doi.org/10.1002/etc.4890

Garnett, J., Halsall, C., Vader, A., Joerss, H., Ebinghaus, R., Leeson, A., & Wynn, P. M. (2021). High Concentrations of Perfluoroalkyl Acids in Arctic Seawater Driven by Early Thawing Sea Ice. *Environmental Science and Technology*, *55*(16), 11049–11059. https://doi.org/10.1021/acs.est.1c01676

Gutiérrez, E. J., Abraham, M. D. R., Baltazar, J. C., Vázquez, G., Delgadillo, E., & Tirado, D. (2020). Pseudomonas fluorescens: A bioaugmentation strategy for oil-contaminated and nutrient-poor soil. *International Journal of Environmental Research and Public Health*, *17*(19), 1–14. https://doi.org/10.3390/ijerph17196959

Harris, J. D., Coon, C. M., Doherty, M. E., McHugh, E. A., Warner, M. C., Walters, C. L., Orahood, O. M., Loesch, A. E., Hatfield, D. C., Sitko, J. C., Almand, E. A., & Steel, J. J. (2022). Engineering and characterization of dehalogenase enzymes from Delftia acidovorans in bioremediation of perfluorinated compounds. *Synthetic and Systems Biotechnology*, *7*(2), 671–676. https://doi.org/10.1016/j.synbio.2022.02.005

Horváthová, H., Lászlová, K., & Dercová, K. (2018). Bioremediation of PCB-contaminated shallow river sediments: The efficacy of biodegradation using individual bacterial strains and their consortia. *Chemosphere*, *193*, 270–277. https://doi.org/10.1016/j.chemosphere.2017.11.012

Hu, F., Wang, P., Li, Y., Ling, J., Ruan, Y., Yu, J., & Zhang, L. (2023). Bioremediation of environmental organic pollutants by Pseudomonas aeruginosa: Mechanisms, methods and challenges. In *Environmental Research* (Vol. 239). Academic Press Inc. https://doi.org/10.1016/j.envres.2023.117211

Hu, M., & Scott, C. (2024). Toward the development of a molecular toolkit for the microbial remediation of per-and polyfluoroalkyl substances. *Applied and Environmental Microbiology*. https://doi.org/10.1128/aem.00157-24

Huang, S., & Jaffé, P. R. (2019). Defluorination of Perfluorooctanoic Acid (PFOA) and Perfluorooctane Sulfonate (PFOS) by Acidimicrobium sp. Strain A6. *Environmental Science and Technology*. https://doi.org/10.1021/acs.est.9b04047

ITRC. (n.d.). *Per-and Polyfluoroalkyl Substances (PFAS) Fact Sheets*.

Jaffé, P. R., Huang, S., Park, J., Ruiz-Urigüen, M., Shuai, W., & Sima, M. (2024). Defluorination of PFAS by Acidimicrobium sp. strain A6 and potential applications for remediation. In *Methods in Enzymology*. Academic Press Inc. https://doi.org/10.1016/bs.mie.2024.01.013

Kato, K., Wong, L. Y., Jia, L. T., Kuklenyik, Z., & Calafat, A. M. (2011). Trends in exposure to polyfluoroalkyl chemicals in the U.S. population: 1999-2008. *Environmental Science and Technology*, *45*(19), 8037–8045. https://doi.org/10.1021/es1043613

Khan, M. F., Chowdhary, S., Koksch, B., & Murphy, C. D. (2023). Biodegradation of Amphipathic Fluorinated Peptides Reveals a New Bacterial Defluorinating Activity and a New Source of Natural Organofluorine Compounds. *Environmental Science and Technology*, *57*(26), 9762–9772. https://doi.org/10.1021/acs.est.3c01240

Kiel, M., & Engesser, K. H. (2015). The biodegradation vs. biotransformation of fluorosubstituted aromatics. In *Applied Microbiology and Biotechnology* (Vol. 99, Issue 18, pp. 7433–7464). Springer Verlag. https://doi.org/10.1007/s00253-015-6817-5

Krafft, M. P., & Riess, J. G. (2015). Selected physicochemical aspects of poly- and perfluoroalkylated substances relevant to performance, environment and sustainability-Part one. *Chemosphere*, *129*, 4–19. https://doi.org/10.1016/j.chemosphere.2014.08.039

Kurihara, T., Yamauchi, T., Ichiyama, S., Takahata, H., & Esaki, N. (2003). Purification, characterization, and gene cloning of a novel fluoroacetate dehalogenase from Burkholderia sp. FA1. *Journal of Molecular Catalysis B: Enzymatic*, *23*(2–6), 347–355. https://doi.org/10.1016/S1381-1177(03)00098-5

Kwon, B. G., Lim, H. J., Na, S. H., Choi, B. I., Shin, D. S., & Chung, S. Y. (2014). Biodegradation of perfluorooctanesulfonate (PFOS) as an emerging contaminant. *Chemosphere*, *109*, 221–225. https://doi.org/10.1016/j.chemosphere.2014.01.072

Lara-Moreno, A., Morillo, E., Merchán, F., Gonzalez-Pimentel, J. L., & Villaverde, J. (2023). Genome sequence of Stenotrophomonas indicatrix CPHE1, a powerful phenanthrene-degrading bacterium. *3 Biotech*, *13*(2). https://doi.org/10.1007/s13205-023-03469-3

Larsen, P. B., & Giovalle, E. (2015). *Perfluoroalkylated substances: PFOA, PFOS and PFOSA : evaluation of health hazards and proposal of a health based quality criterion for drinking water, soil and ground water*. The Danish Environmental Protection Agency.

Leong, L. E. X., Khan, S., Davis, C. K., Denman, S. E., & McSweeney, C. S. (2017). Fluoroacetate in plants - a review of its distribution, toxicity to livestock and microbial detoxification. In *Journal of Animal Science and Biotechnology* (Vol. 8, Issue 1). BioMed Central Ltd. https://doi.org/10.1186/s40104-017-0180-6

Lewis, M., Kim, M. H., Liu, E. J., Wang, N., & Chu, K. H. (2016). Biotransformation of 6:2 polyfluoroalkyl phosphates (6:2 PAPs): Effects of degradative bacteria and co-substrates. *Journal of Hazardous Materials*, *320*, 479–486. https://doi.org/10.1016/j.jhazmat.2016.08.036

Li, J., Ou, Y., Wang, L., Zheng, Y., Xu, W., Peng, J., Zhang, X., Cao, Z., & Ye, J. (2024). Responses of a polycyclic aromatic hydrocarbon-degrading bacterium, Paraburkholderia fungorum JT-M8, to Cd (II) under P-limited oligotrophic conditions. *Journal of Hazardous Materials*, *465*. https://doi.org/10.1016/j.jhazmat.2023.133123

Li, Y., Yue, Y., Zhang, H., Yang, Z., Wang, H., Tian, S., Wang, J. bo, Zhang, Q., & Wang, W. (2019). Harnessing fluoroacetate dehalogenase for defluorination of fluorocarboxylic acids: in silico and in vitro approach. *Environment International*, *131*. https://doi.org/10.1016/j.envint.2019.104999

Lindstrom, A. B., Strynar, M. J., & Libelo, E. L. (2011). Polyfluorinated compounds: Past, present, and future. *Environmental Science and Technology*, *45*(19), 7954–7961. https://doi.org/10.1021/es2011622

Liu, J., & Mejia Avendaño, S. (2013). Microbial degradation of polyfluoroalkyl chemicals in the environment: A review. In *Environment International* (Vol. 61, pp. 98–114). Elsevier Ltd. https://doi.org/10.1016/j.envint.2013.08.022

Mahoney, H., Xie, Y., Brinkmann, M., & Giesy, J. P. (2022). Next generation per- and poly-fluoroalkyl substances: Status and trends, aquatic toxicity, and risk assessment. In *Eco-Environment and Health* (Vol. 1, Issue 2, pp. 117–131). Elsevier B.V. https://doi.org/10.1016/j.eehl.2022.05.002

Nielsen, T. K., Browne, P. D., & Hansen, L. H. (2022). Antibiotic resistance genes are differentially mobilized according to resistance mechanism. *GigaScience*, *11*. https://doi.org/10.1093/gigascience/giac072

OECD. (2021). *Reconciling Terminology of the Universe of Per-and Polyfluoroalkyl Substances: Recommendations and Practical Guidance Series on Risk Management No.61 JT03479350 OFDE*.

Parales, R. E., Luu, R. A., Chen, G. Y., Liu, X., Wu, V., Lin, P., Hughes, J. G., Nesteryuk, V., Parales, J. V., & Ditty, J. L. (2013). Pseudomonas putida F1 has multiple chemoreceptors with overlapping specificity for organic acids. *Microbiology (United Kingdom)*, *159*(PART 6), 1086–1096. https://doi.org/10.1099/mic.0.065698-0

Parsons, J. R., Sáez, M., Dolfing, J., & De Voogt, P. (2008). *Reviews of Environmental Contamination and Toxicology Vol 196* (D. M. Whitacre, Ed.; Vol. 196). Springer US. https://doi.org/10.1007/978-0-387-78444-1

Region Sjælland. (2023, June 15). *PFAS-testcenter på tidligere Korsør Brandskole*.

Region Slagelse Kommune. (2021). *PFOS Korsør Sit Plan-Proeveudtagning*.

Rekik, H., Arab, H., Pichon, L., El Khakani, M. A., & Drogui, P. (2024). Per-and polyfluoroalkyl (PFAS) eternal pollutants: Sources, environmental impacts and treatment processes. In *Chemosphere* (Vol. 358). Elsevier Ltd. https://doi.org/10.1016/j.chemosphere.2024.142044

Routti, H., Aars, J., Fuglei, E., Hanssen, L., Lone, K., Polder, A., Pedersen, Å. O., Tartu, S., Welker, J. M., & Yoccoz, N. G. (2017). Emission Changes Dwarf the Influence of Feeding Habits on Temporal Trends of Per- and Polyfluoroalkyl Substances in Two Arctic Top Predators. *Environmental Science and Technology*, *51*(20), 11996–12006. https://doi.org/10.1021/acs.est.7b03585

Schrenk, D., Bignami, M., Bodin, L., Chipman, J. K., del Mazo, J., Grasl-Kraupp, B., Hogstrand, C., Hoogenboom, L., Leblanc, J. C., Nebbia, C. S., Nielsen, E., Ntzani, E., Petersen, A., Sand, S., Vleminckx, C., Wallace, H., Barregård, L., Ceccatelli, S., Cravedi, J. P., … Schwerdtle, T. (2020). Risk to human health related to the presence of perfluoroalkyl substances in food. *EFSA Journal*, *18*(9). https://doi.org/10.2903/j.efsa.2020.6223

Seong, H. J., Kwon, S. W., Seo, D. C., Kim, J. H., & Jang, Y. S. (2019). Enzymatic defluorination of fluorinated compounds. In *Applied Biological Chemistry* (Vol. 62, Issue 1). Springer Science and Business Media B.V. https://doi.org/10.1186/s13765-019-0469-6

Shahsavari, E., Rouch, D., Khudur, L. S., Thomas, D., Aburto-Medina, A., & Ball, A. S. (2021). Challenges and Current Status of the Biological Treatment of PFAS-Contaminated Soils. In *Frontiers in Bioengineering and Biotechnology* (Vol. 8). Frontiers Media S.A. https://doi.org/10.3389/fbioe.2020.602040

Starling, A. P., Liu, C., Shen, G., Yang, I. V., Kechris, K., Borengasser, S. J., Boyle, K. E., Zhang, W., Smith, H. A., Calafat, A. M., Hamman, R. F., Adgate, J. L., & Dabelea, D. (2020). Prenatal exposure to per-and polyfluoroalkyl substances, umbilical cord blood DNA methylation, and cardio-metabolic indicators in newborns: The healthy start study. *Environmental Health Perspectives*, *128*(12), 1–7. https://doi.org/10.1289/EHP6888

Thacharodi, A., Hassan, S., Singh, T., Mandal, R., Chinnadurai, J., Khan, H. A., Hussain, M. A., Brindhadevi, K., & Pugazhendhi, A. (2023). Bioremediation of polycyclic aromatic hydrocarbons: An updated microbiological review. *Chemosphere*, *328*. https://doi.org/10.1016/j.chemosphere.2023.138498

Thermo Scientific. (2015). *Measuring Fluoride in Water and Wastewater using the Thermo Scientific Orion Dual Star pH/ISE Meter*.

Tvede, I., & Frandsen, M. (2023, December 25). *Massive mørketal for virksomheders brug af PFAS: 'Vi får aldrig et overblik'*. DR.

Vendl, C., Taylor, M. D., Bräunig, J., Ricolfi, L., Ahmed, R., Chin, M., Gibson, M. J., Hesselson, D., Neely, G. G., Lagisz, M., & Nakagawa, S. (2024). Profiling research on PFAS in wildlife: Systematic evidence map and bibliometric analysis. *Ecological Solutions and Evidence*, *5*(1). https://doi.org/10.1002/2688-8319.12292

Wackett, L. P. (2021). Nothing lasts forever: understanding microbial biodegradation of polyfluorinated compounds and perfluorinated alkyl substances. In *Microbial Biotechnology* (Vol. 15, Issue 3, pp. 773–792). John Wiley and Sons Ltd. https://doi.org/10.1111/1751-7915.13928

Wackett, L. P. (2024). Evolutionary obstacles and not C–F bond strength make PFAS persistent. *Microbial Biotechnology*, *17*(4). https://doi.org/10.1111/1751-7915.14463

Wang, Z., Dewitt, J. C., Higgins, C. P., & Cousins, I. T. (2017). A Never-Ending Story of Per- and Polyfluoroalkyl Substances (PFASs)? *Environmental Science and Technology*, *51*(5), 2508–2518. https://doi.org/10.1021/acs.est.6b04806

Wu, L., & Deng, H. (2020). Defluorination of 4-fluorothreonine by threonine deaminase. *Organic and Biomolecular Chemistry*, *18*(32), 6236–6240. https://doi.org/10.1039/d0ob01358g

Xiao, J., Huang, J., Wang, Y., & Qian, X. (2023). The fate and behavior of perfluorooctanoic acid (PFOA) in constructed wetlands: Insights into potential removal and transformation pathway. *Science of the Total Environment*, *861*. https://doi.org/10.1016/j.scitotenv.2022.160309

Xiao, Y., Jiang, R., Wu, X., Zhong, Q., Li, Y., & Wang, H. (2021). Comparative Genomic Analysis of Stenotrophomonas maltophilia Strain W18 Reveals Its Adaptative Genomic Features for Degrading Polycyclic Aromatic Hydrocarbons. *Microbiology Spectrum*, *9*(3). https://doi.org/10.1128/spectrum.01420-21

Xu, G., Zhao, S., Liu, J., & He, J. (2023). Bioremediation of organohalide pollutants: progress, microbial ecology, and emerging computational tools. In *Current Opinion in Environmental Science and Health* (Vol. 32). Elsevier B.V. https://doi.org/10.1016/j.coesh.2023.100452

Yi, L. B., Chai, L. Y., Xie, Y., Peng, Q. J., & Peng, Q. Z. (2016). Isolation, identification, and degradation performance of a PFOA-degrading strain. *Genetics and Molecular Research*, *15*(2). https://doi.org/10.4238/gmr.15028043

Zylstra, G. J., Mccombie, W. R., Gibson, D. T., & Finette, B. A. (1988). Toluene Degradation by Pseudomonas putida Fl: Genetic Organization of the tod Operon. In *APPLIED AND ENVIRONMENTAL MICROBIOLOGY* (Vol. 54, Issue 6).

Supplementary Materials

Potential Degradation Pathways for PFOA

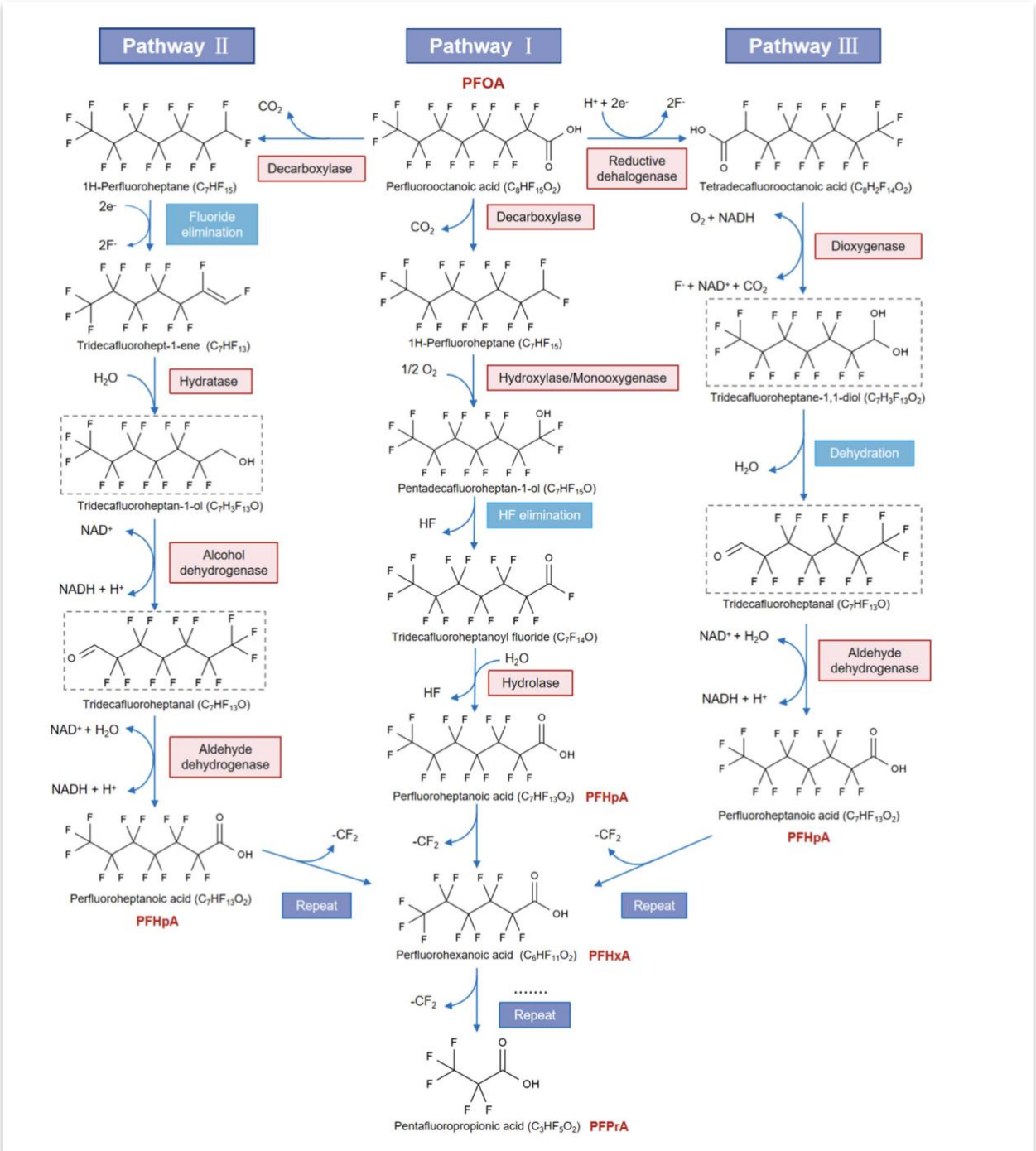

Figure 11: Degradation pathway of PFOA by CW as described in The Fate and Behavior of Perfluorooctanoic Acid (PFOA) in Constructed Wetlands: Insights into Potential Removal and Transformation Pathway (J. Xiao et al., 2023).

Original Chemical Analysis Results

	PFOA	13C-PFOA	PFHpA	PFHxA
SolventBlank	0	7.00E+08		
Plastic control	0	6.00E+08		
Control	3.50E+09	4.40E+08	x	x
3B	1.60E+09	5.60E+08		
3C	1.80E+09	4.80E+08		
3E	2.00E+09	4.70E+08		
6B	1.00E+09	5.40E+08		
10A	1.60E+09	5.70E+08		
10B	1.70E+09	5.70E+08		
8A	1.20E+09	6.80E+08		
8F	1.10E+09	6.40E+08		
8G	1.20E+09	5.70E+08		
5A	1.20E+09	6.50E+08		
5B	1.20E+09	6.50E+08		
5C	1.20E+09	6.10E+08		
5D	1.20E+09	6.60E+08		
5E	1.20E+09	5.90E+08		
5F	1.20E+09	5.80E+08		
5G	1.20E+09	5.90E+08		
5H	1.30E+09	5.80E+08		
SolventBlank	0	7.00E+08		
SolventBlank	0	7.00E+08		

Table 13: Results from LC-HRMS/MS.

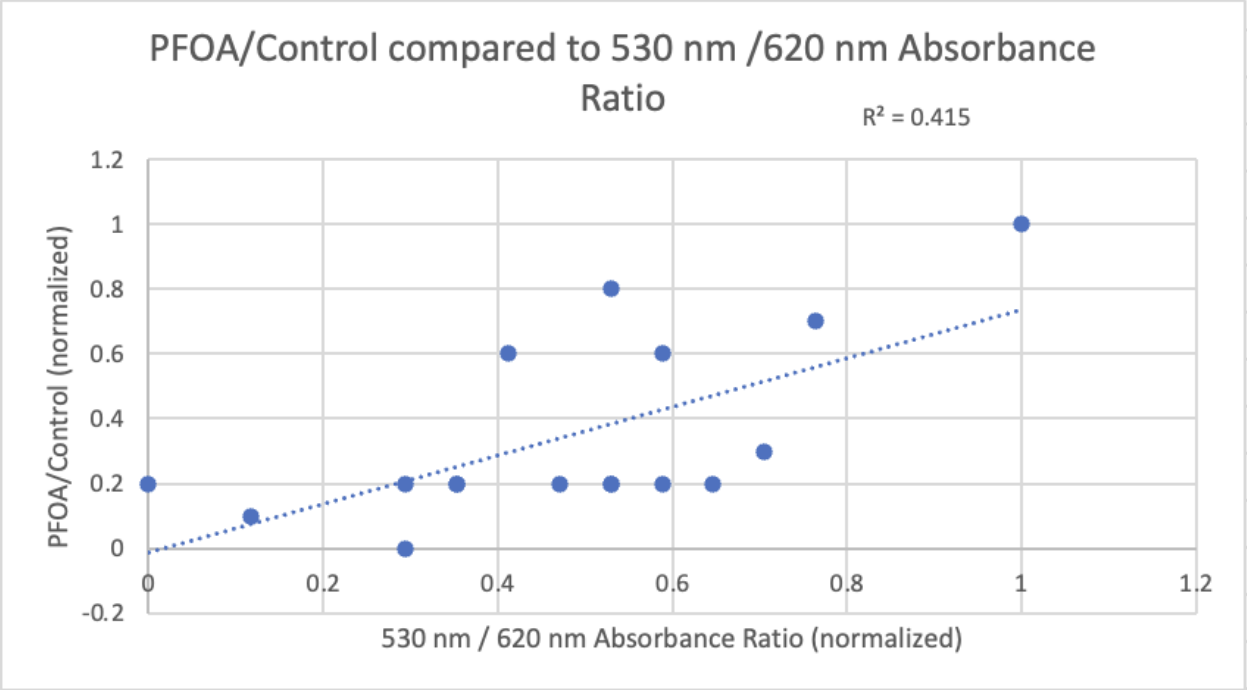

Figure 12: PFOA compared to control for each sample point plotted against the respective 530 nm / 620 nm absorbance ratio.

Ratio of Compound to Internal Standard and Comparison to Control for PFOA

Sample	Ratio Compound/IS	Diff from Control
cLC_neg_GenPFOA_3B	2.805780926	0.344219302
cLC_neg_GenPFOA_3C	3.784827457	0.464330858
cLC_neg_GenPFOA_3E	4.17371406	0.512040311
cLC_neg_GenPFOA_5A	1.855288418	0.227610815
cLC_neg_GenPFOA_5B	1.874924494	0.230019811
cLC_neg_GenPFOA_5C	2.062366295	0.253015579
cLC_neg_GenPFOA_5D	1.808425396	0.221861558
cLC_neg_GenPFOA_5E	2.054082317	0.251999283
cLC_neg_GenPFOA_5F	2.155723411	0.264468833
cLC_neg_GenPFOA_5G	2.048359387	0.251297181
cLC_neg_GenPFOA_5H	2.223536901	0.272788339
cLC_neg_GenPFOA_6B	1.920993682	0.23567168
cLC_neg_GenPFOA_8A	1.749491112	0.214631372
cLC_neg_GenPFOA_8F	1.737763669	0.213192623
cLC_neg_GenPFOA_8G	2.012637215	0.246914707
cLC_neg_GenPFOA_10A	2.696533573	0.330816599
cLC_neg_GenPFOA_10B	2.942866171	0.361037217
cLC_neg_GenPFOA_PlasticControl		
cLC_neg_GenPFOA_PositiveControl	8.15114351	
cLC_neg_GenPFOA_SolventBlank		
cLC_neg_GenPFOA_SolventBlank_20240508200650		
cLC_neg_GenPFOA_SolventBlank_20240508203744		

Table 14: Ratio of areas found by LC-HRMS/MS for PFOA to the internal standard and the difference per sample when compared to the control.

Ratio of Compound to Internal Standard and Comparison to Control for PFHxA

Sample	Ratio Compound/IS	Diff from Control
cLC_neg_GenPFOA_3B	0.011898849	0.500150266
cLC_neg_GenPFOA_3C	0.019968853	0.839360779
cLC_neg_GenPFOA_3E	0.018512143	0.778130156
cLC_neg_GenPFOA_5A	0.008466486	0.355876033
cLC_neg_GenPFOA_5B	0.006580521	0.276602315
cLC_neg_GenPFOA_5C	0.008717234	0.366415835
cLC_neg_GenPFOA_5D	0.007878735	0.331170819
cLC_neg_GenPFOA_5E	0.007526704	0.316373698
cLC_neg_GenPFOA_5F	0.008645425	0.363397479
cLC_neg_GenPFOA_5G	0.007374869	0.309991567
cLC_neg_GenPFOA_5H	0.009122276	0.383441193
cLC_neg_GenPFOA_6B	0.010286076	0.432359785
cLC_neg_GenPFOA_8A	0.008229363	0.345908921
cLC_neg_GenPFOA_8F	0.007325759	0.307927281
cLC_neg_GenPFOA_8G	0.008096148	0.340309434
cLC_neg_GenPFOA_10A	0.012148364	0.510638269
cLC_neg_GenPFOA_10B	0.014422188	0.606215028
cLC_neg_GenPFOA_PlasticControl		
cLC_neg_GenPFOA_PositiveControl	0.023790548	
cLC_neg_GenPFOA_SolventBlank		
cLC_neg_GenPFOA_SolventBlank_20240508200650		
cLC_neg_GenPFOA_SolventBlank_20240508203744		

Table 15: Ratio of areas found by LC-HRMS/MS for PFHxA to the internal standard and the difference per sample when compared to the control.

Difference from control per sample for PFHpA

Sample	Difference from Control
cLC_neg_GenPFOA_3B	0.49611574
cLC_neg_GenPFOA_3C	0.745736241
cLC_neg_GenPFOA_3E	0.811140816
cLC_neg_GenPFOA_5A	0.396852611
cLC_neg_GenPFOA_5B	0.343170624
cLC_neg_GenPFOA_5C	0.372279305
cLC_neg_GenPFOA_5D	0.303587641
cLC_neg_GenPFOA_5E	0.349757704
cLC_neg_GenPFOA_5F	0.402055176
cLC_neg_GenPFOA_5G	0.368295622
cLC_neg_GenPFOA_5H	0.411227885
cLC_neg_GenPFOA_6B	0.383457605
cLC_neg_GenPFOA_8A	0.383295144
cLC_neg_GenPFOA_8F	0.351006413
cLC_neg_GenPFOA_8G	0.370686424
cLC_neg_GenPFOA_10A	0.518236687
cLC_neg_GenPFOA_10B	0.51457285
cLC_neg_GenPFOA_PlasticControl	
cLC_neg_GenPFOA_PositiveControl	
cLC_neg_GenPFOA_SolventBlank	
cLC_neg_GenPFOA_SolventBlank_20240508200650	
cLC_neg_GenPFOA_SolventBlank_20240508203744	

Table 16: Areas found by LC-HRMS/MS for PFHpA the difference per sample when compared to the control.

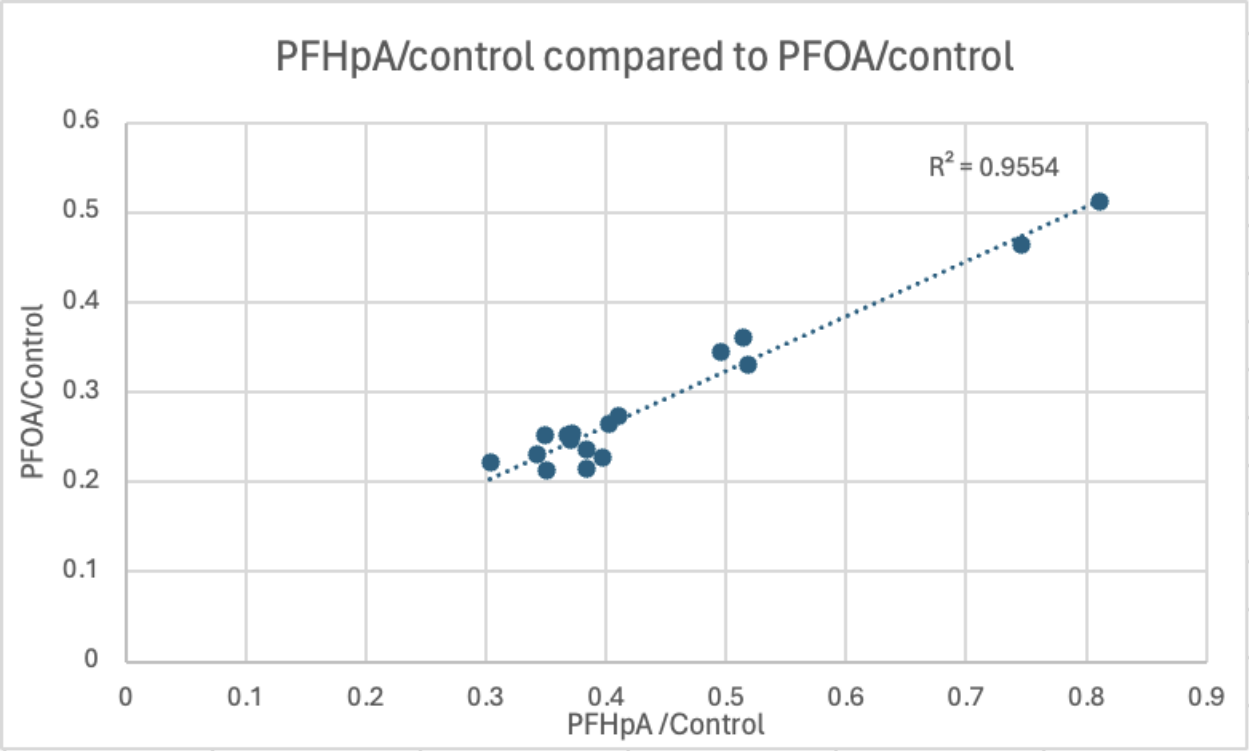

Figure 13: Difference in PFHpA measured in samples as compared to control and difference in PFOA measured in samples compared to control plotted against each other.

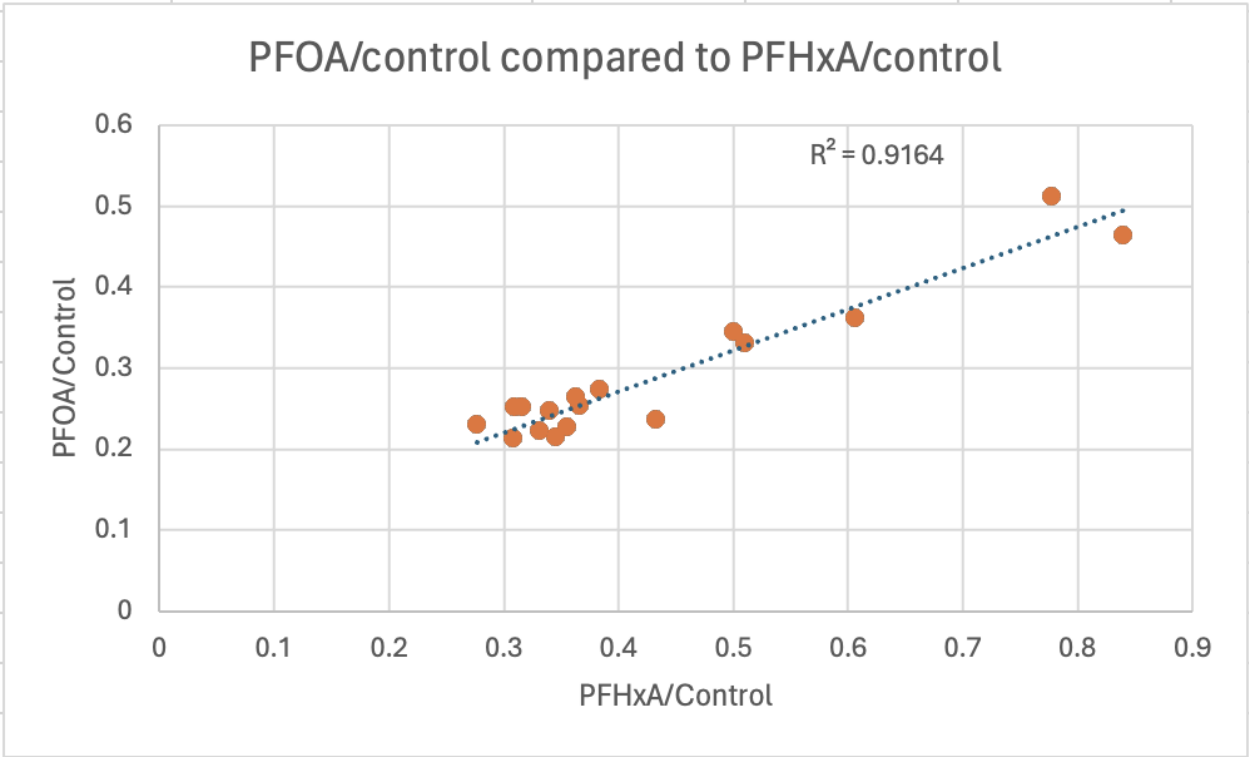

Figure 14: Difference in PFHxA measured in samples as compared to control and difference in PFOA measured in samples compared to control plotted against each other.

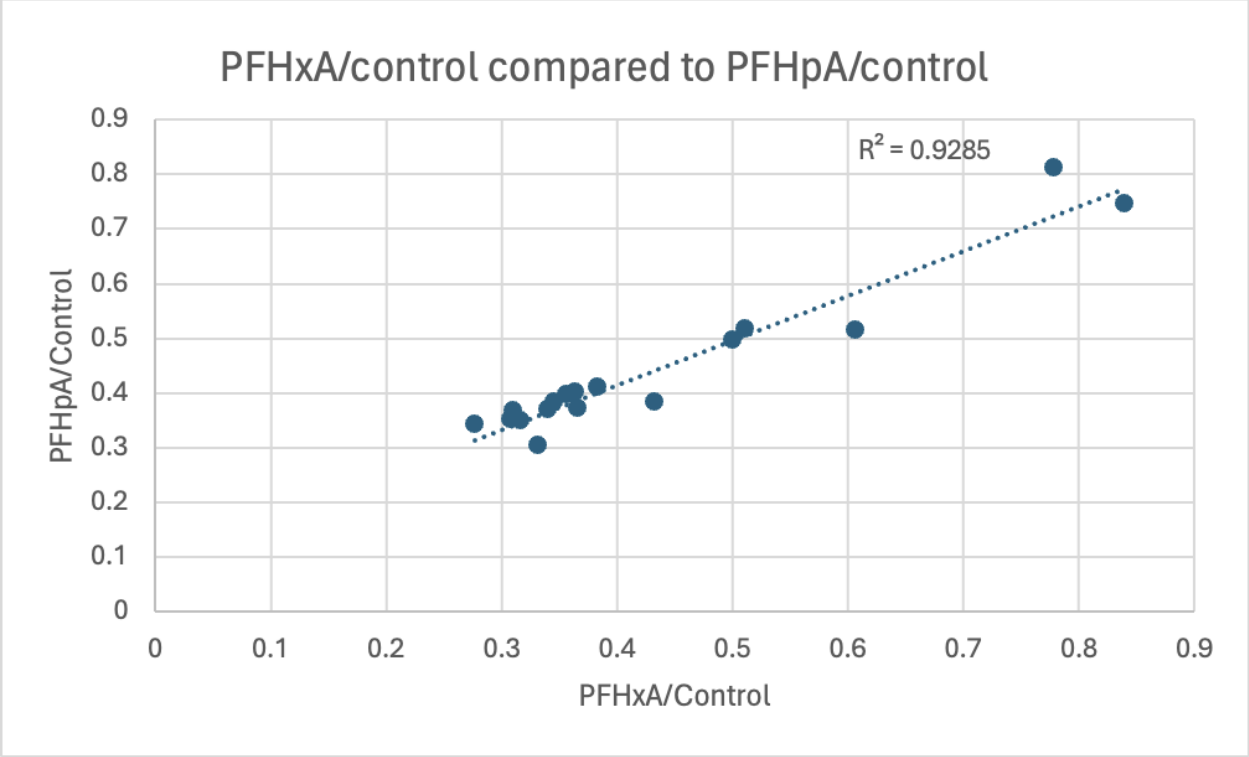

Figure 15: Difference in PFHxA measured in samples as compared to control and difference in PFHpA measured in samples compared to control plotted against each other.

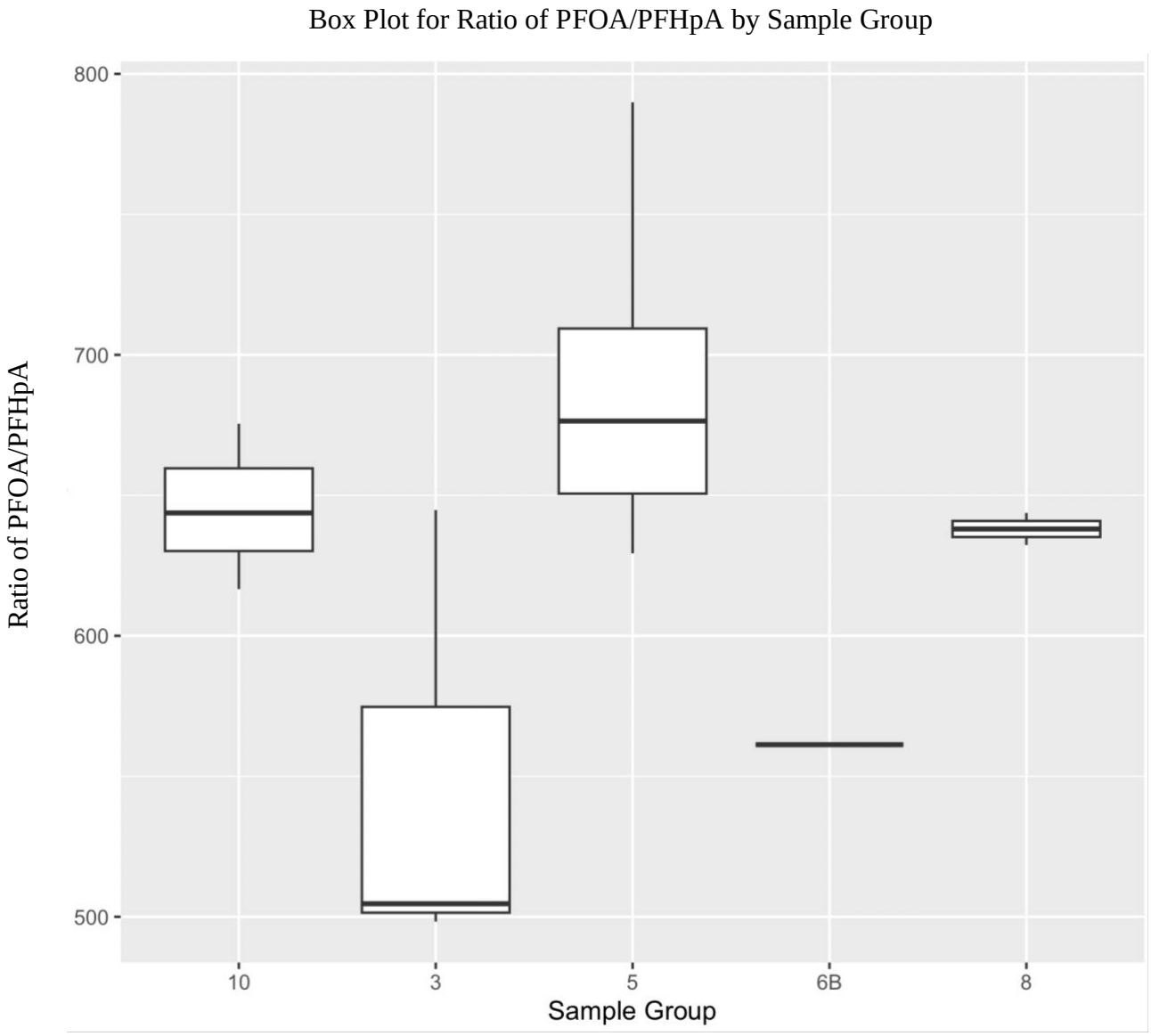

Figure 16: Box Plot for Ratio of PFOA/PFHpA by Sample Group

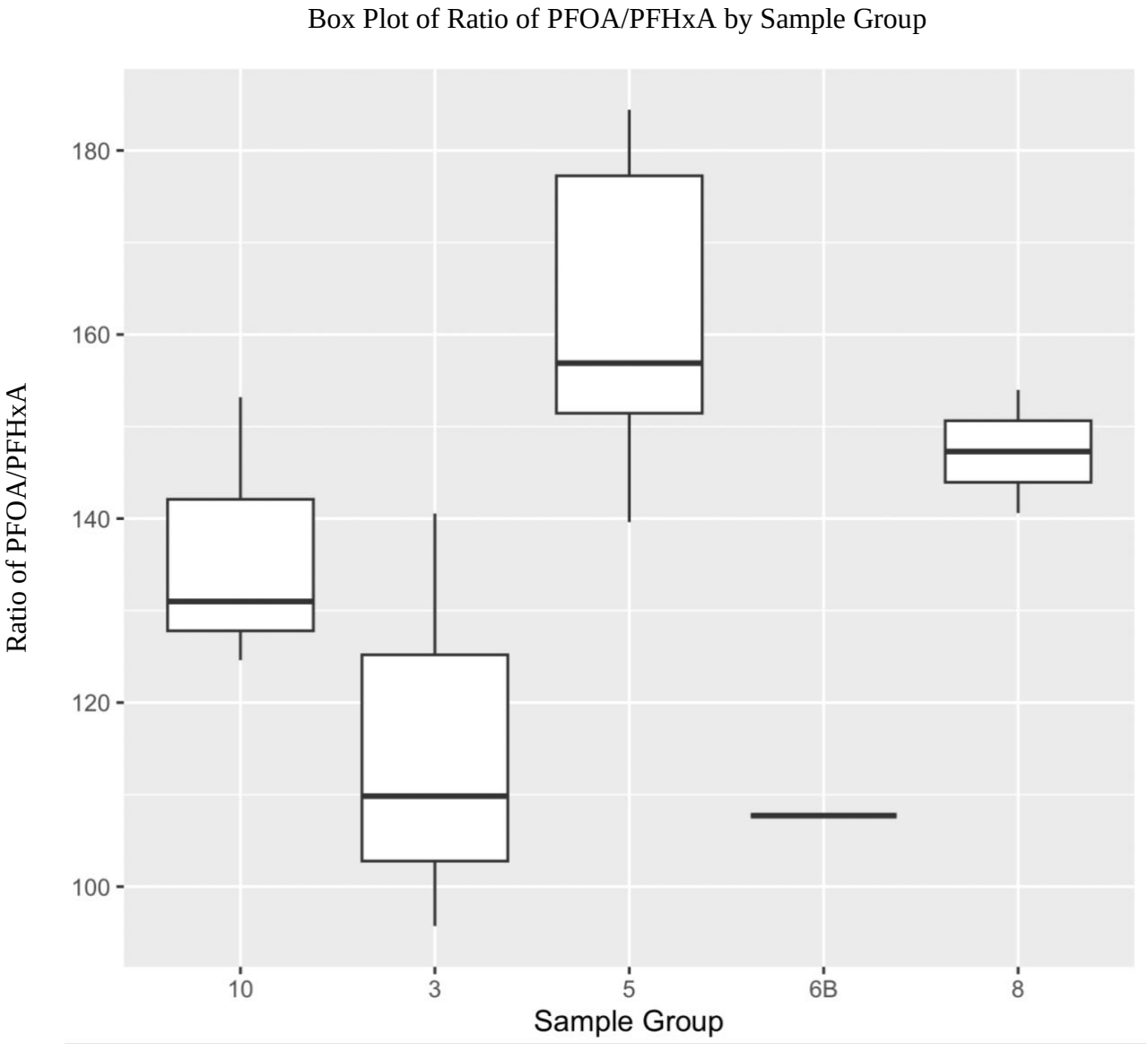

Figure 17: Box Plot for Ratio of PFOA/PFHxA by Sample Group